Research Square

Preprints are preliminary reports that have not undergone peer review.
They should not be considered conclusive, used to inform clinical practice,
or referenced by the media as validated information.

Polysaccharide from Phormidium persicinum (Reinke) Gom. promotes neuronal differentiation and mitigates hypoxia-induced neuronal disruptions in vitro

Sanjivani Satpute
KET's V. G. Vaze College (Empowered Autonomous)
Thangajyothi Nadar
KET's V. G. Vaze College (Empowered Autonomous)
Kishan Kannaujiya
KET's V. G. Vaze College (Empowered Autonomous)
Akshay Bagwe
akshaybagwe@vazecollege.net
KET's V. G. Vaze College (Empowered Autonomous)
Manjushri Deodhar
KET's V. G. Vaze College (Empowered Autonomous)
Bharatbhushan Sharma
KET's V. G. Vaze College (Empowered Autonomous)

Research Article

Keywords: Microalgae, Uronic acids, SH-SY5Y, Dopamine, neurodifferentiation

Posted Date: October 23rd, 2026

DOI: https://doi.org/10.21203/rs.3.rs-11252971/v1

License: This work is licensed under a Creative Commons Attribution 4.0 International License.
Read Full License

Additional Declarations: No competing interests reported.

Polysaccharide from *Phormidium persicinum* (Reinke) Gom. promotes neuronal differentiation and mitigates hypoxia-induced neuronal disruptions *in vitro*

Sanjivani Satpute[1], Thangajyothi Nadar[1], Kishan Kannaujiya[1], Akshay Bagwe[1]*, Manjushri Deodhar[2] and Bharatbhushan Sharma[1]

[1]Department of Zoology, KET's V. G. Vaze College (Empowered Autonomous), Mumbai - 400081, Maharashtra, India

[2]Department of Botany, KET's V. G. Vaze College (Empowered Autonomous), Mumbai - 400081, Maharashtra, India

*Email: akshaybagwe@vazecollege.net

Address of Corresponding Author:
Dr. Akshay Dilip Bagwe.
Assistant Professor, Department of Zoology,
KET's V. G. Vaze College (Empowered Autonomous),
Mithagar Road, Mumbai - 400081, Maharashtra, India

Abstract:

Hypoxia is an important pathogenic factor affecting cellular metabolism and neurogenesis in neurological disorders. Neuronal stem cells (NSCs) are particularly sensitive to oxygen deprivation because they depend on tightly regulated metabolic programs during differentiation. Microalgal polysaccharides have recently gained interest due to their cytoprotective, anti-inflammatory, and antioxidant properties, but their potential to prevent hypoxia-induced metabolic stress in neural lineage commitment is poorly understood. Therefore, the present study evaluates the potential of crude polysaccharide derived from an indigenous marine microalga to attenuate metabolic perturbations in differentiating NSCs exposed to chemical hypoxia. The crude polysaccharide was extracted from *Phormidium persicinum* (Reinke) Gom. and characterized for its biochemical components. The compositional analysis revealed the presence of 24.35% sulphate, 16.69% carbohydrates, 12.66% uronic acids, and 3.77% protein along with monosaccharides like rhamnose, xylose, galactose, and fucose. Also, the impact of polysaccharide on the outcomes of neuronal differentiation was investigated *in vitro* on human neuronal stem cells (SH-SY5Y) under cobalt chloride induced hypoxia stress. The treatment with polysaccharide at a concentration of 50 $\mu g\ mL^{-1}$ supplemented with retinoic acid in the ratio of 80:20 induced a sustained formation of neurite outgrowth accompanied by metabolic stabilizations after differentiation. Furthermore, treatment with polysaccharide under hypoxic conditions promotes a more favourable metabolic profile, as reported by optimal levels of dopamine, epinephrine, serotonin, acetylcholinesterase, and adenosine triphosphatase. The study underscores the promising nature of novel algal polysaccharide for the treatment of neurodegenerative disorders and suggests further investigations to purify and pinpoint its bioactive components.

Keywords: Microalgae, Uronic acids, SH-SY5Y, Dopamine, neurodifferentiation

Introduction:

Neurodegenerative diseases are a diverse group of disorders marked by gradual and selective loss of neurons leading to deficits in sensation, motor function, and cognition, as observed in Parkinson's disease (PD), Huntington's disease (HD), amyotrophic lateral sclerosis (ALS), and multiple sclerosis (MS) [1,2,3]. Hypoxia-mediated brain injury is one of the significant contributors to neurodegenerative disorders [4, 5]. Decreased levels of oxygen to the brain causes substantial metabolic change in neuronal and non-neural cells. Initially, it causes rapid alterations in membrane lipid composition and enzymatic activity, followed by sustained modifications in gene expression and protein synthesis. These processes are widely regarded as key contributors to cognitive decline, seizures, and various other neurological impairments. Current data suggests that vascular factors and decreased cerebral oxygen availability contribute to the pathogenesis of several neurodegenerative disorders and may further influence their progression [6]. These diseases are life threatening for the patients, moreover they also impose economic burden on both family and society [7]. The majority of current treatments employed for these diseases alleviate symptoms and may modestly slow disease progression, but they do not cure the underlying condition [8, 9].

Nerve repair and regeneration therapy is a promising treatment for neurological diseases. Extensive amounts of study has been done in the area, from endogenous and exogenous aspects to aid nerve repair and regeneration [10]. Within regenerative medicine, neural stem cells therapy represent a promising approach for addressing neurodegenerative disorders [11]. Neural stem cells (NSCs) are multipotent cells characterised by their strong self-renewal capacity and ability to differentiate into varied cells such as, neuronal and glial cells [12, 13]. However, directly transplanted NSCs face major limitations such as low survival and irrational differentiation [14,15,16,17]. Endogenous neurogenesis moderated by NSCs leads to various pathological conditions, like epilepsy, multiple sclerosis, ischemic stroke, and Alzheimer's disease and it is not enough alone [18, 19]. To address the limitations associated with direct NSC transplantation, particularly in neurodegenerative diseases characterized by the loss of specific cell populations, considerable efforts have focused on manipulating NSC fate prior to transplantation to direct terminal differentiation and facilitate targeted cell replacement [20, 21]. This underscores the need for the discovery of compounds that can induce differentiation of NSCs exogenously without disrupting their cellular homeostasis.

Algal polysaccharides are polymers with high molecular weight extracted from macroalgae and microalgae. They serve as abundant reservoirs of biological activity owing to their distinctive structural features. Their functional properties like antioxidant, antiviral, anti-inflammatory, and antitumor effects are largely determined by their structural complexity, monosaccharide composition, molecular weight, and specifically, their degree of sulfation [22]. Moreover, they are non-toxic, highly biocompatible with minimal side effects. These properties make them an auspicious biomolecule for developing novel therapeutics that are applicable through numerous pathways or offer additional therapeutic benefits when used alongside standard treatment regimens. Consequently, natural polysaccharides are emerging as promising mitigators for combating neurodegenerative diseases such as Alzheimer's Disease (AD), PD and ALS [23]. These polysaccharides act as neuroprotective agents for inflammation modulation and endogenous antioxidant pathways. They also significantly improved the morphophysiological characteristics of the nervous system under stress conditions. Thus, they may offer therapeutic benefits in neurodegenerative disorders linked to basal ganglia impairment. Recent discoveries have established that polysaccharides extracted from marine organisms and their derivatives show significant potential in the management of neurodegenerative diseases [24]. Notably, a polysaccharide derived from green algae has been reported to exhibit anti-Parkinson's disease activity by inhibiting α-synuclein fibrillation [25, 26]. Therefore, studying algae for neuroprotective polysaccharides allows researchers to assess the potential of these compounds to develop unique systems for prevention and treatment of neurodegenerative diseases. Furthermore, these molecules may also show potential for overcoming the challenges of current treatments [27].

Therefore, the present study aimed to investigate the protective potential of crude exopolysaccharide extracted from the indigenous marine alga *Phormidium persicinum* against hypoxia-induced neuronal injury in human neuronal stem (SH-SY5Y) cells *in vitro*. The chemical composition of the extracted polysaccharide was analysed and evaluated for its ability to promote differentiation in neuronal stem cells. Furthermore, the protective potential of the polysaccharide against hypoxia-induced metabolic disturbances in neuronal stem cells was evaluated by analysing neurotransmitter and neuroenzyme levels.

Materials and Methods:

Cultivation of *Phormidium persicinum*

The unialgal culture of *Phormidium persicinum* was isolated from the salt pans of eastern suburbs of Mumbai, Maharashtra, India (19°09'06.8"N 72°57'31.9"E) and authenticated from National Repository for Microalgae & Cyanobacteria (Freshwater & Marine), Bharatidasan University, Tiruchirapalli. About 0.5 gm L^{-1} of inoculum was cultivated in an 18 L flat panel glass photobioreactor containing sea-water BG-11 medium and maintained at outdoor conditions under constant aeration. The semicontinuous culturing method was adopted wherein, after every 4 days, biomass from 1 L of culture was harvested for polysaccharide extraction and replaced with 1 L of fresh medium. The harvesting was performed 10 times during the period of 40 days and polysaccharide was extracted from each harvest separately.

Extraction of *Phormidium persicinum* polysaccharide (PS)

The extraction of polysaccharide was performed by the freeze-thaw method as described earlier [28] with slight modifications. The freshly harvested wet biomass was heated with distilled water (1:1 v/v) in a hot-water bath at 80º C for 1 h. After slight cooling, the material was centrifuged at 6000 RPM for 10 mins and supernatant was aspirated. The ethanol was added in the supernatant at the ratio 1:1 (v/v) and the mixture was kept at - 4ºC overnight. The polysaccharide layer was scooped out and dried at 60º C.

Estimation of total carbohydrate content

The total carbohydrate content was estimated as described previously [29] with some modifications. The reaction mixture consisting of 40 µL of PS (1 mg mL^{-1}) and 200 µL of anthrone reagent was incubated in a boiling water bath for 10 mins. It was allowed to cool to room temperature for colour development. The absorbance was measured at 630 nm ELISA microplate reader and the total carbohydrate content was calculated from the standard curve plotted using glucose.

Estimation of total protein content

The total protein content was determined as described earlier [30] with slight modifications. The reaction mixture containing 100 µL of PS (1 mg mL^{-1}), 100 µL phosphate buffer (pH 7.4) and 5 mL alkaline copper sulphate was incubated at room temperature for 15 mins followed by the addition of 500 µL Folin-C reagent. The absorbance was taken at 660 nm on UV-VIS spectrophotometer and total protein content was calculated from the standard curve plotted using bovine serum albumin.

Estimation of sulphate content

The total sulphate content was determined as described previously [31] with some modifications. Briefly, 4 mg of PS was dissolved in 1 mL of 1 M HCl and heated at 100°C for 5 h. The mixture was cooled to room temperature and was diluted with 1 mL distilled water. The reaction mixture containing 114 µL of the sample, 79 µL of 3% trichloroacetic acid, and 57 µL of barium chloride–gelatin reagent was incubated at room temperature for 30 mins. The absorbance was measured at 420 nm and the sulfate content was calculated from the standard curve plotted using sodium sulphate.

Estimation of uronic acid content

The uronic acid content was estimated as described earlier [32] with some modifications. The reaction mixture containing 35 µL of PS (1 mg mL^{-1}) and 211 µL of disodium tetraborate–sulfuric acid solution was incubated in a boiling water bath for 5 mins. The mixture was cooled immediately and 3.5 µL of 0.15% m-hydroxydiphenyl NaOH was added for colour development. The absorbance was measured at 520 nm ELISA microplate reader and the uronic acid content was calculated from the standard curve plotted using glucuronic acid.

GC-MS analysis for determination of monosaccharides

The determination of monosaccharide was performed as described previously [33] with some modifications. The PS solution (2 mg mL^{-1}, 100 µL) was mixed with 100 µL of 4 M trifluoroacetic acid and hydrolyzed at 100°C for 8 h. After cooling to room temperature, the reduction of hydrolysate was carried out by adding freshly prepared sodium borohydride solution and kept at room temperature for 12 h. 100 µL of D-myoinositol (1.8 mg mL^{-1}) was added to the mixture which was then treated with 100 µL liquid pyridine and 100 µL BSTFA for formation of trimethylsilyl derivatives. 1 µL of derivatized sample was dissolved in 100 µL dichloromethane and loaded into the GC system (Chromatec-Crystal 5000) in splitless mode. The monosaccharides were separated on a C-18 column under programmed temperature conditions and quantified in Flame ionization detector (FID) using mass-to-charge ratios data available from the MS library.

Cell culture

Human neuroblastoma cell line (SH-SY5Y) (Epithelial, ATCC HTB-11) was chosen because of its wide-ranging applications in neurobiology and its utility as a model system for studying neurological disorders. The cells were obtained from the National Centre for Cell Sciences, Pune, India and were cultured in Dulbecco's modified Eagle's medium (DMEM) supplemented with

10% heat-inactivated fetal bovine serum (FBS), gentamicin, and additional medium supplements. Cultures were maintained in sterile 25 cm^2 T-flasks at 37°C in a humidified incubator with 5% CO_2. The viability of cells was counted using the trypan blue dye exclusion method [34]. The stem cells were treated with 10 µM retinoic acid for 24 h to induce differentiation whenever required [35].

Differentiation potential of PS

Human neuroblastoma stem cells were seeded at the concentration of 1×10^5 cells/mL in each well of 96 well plate. The cells were then treated with PS at the concentrations of 6.25, 12.5, 25, 50 and 100 µg/mL for 24, 48 and 72 h. The 10 µM of retinoic acid was used as a positive control for each set of experiments. At the end of the exposure, neurite outgrowth assay was performed and mitochondrial dehydrogenase activity was measured as markers for neuronal differentiation. The concentration of PS that showed highest differentiation potential was determined and new batches of cells were incubated with PS and 10 µM retinoic acid in the ratios of 100:0, 80:20, 60:40, 40:60, 20:80 and 0:100 for 48 h. These cells were then assessed for morphological and biochemical markers of differentiation.

Effect of PS under hypoxia

The chemical hypoxia was induced in the SH-SY5Y cell line by treating the cells with different concentrations of cobalt chloride ($CoCl_2$) [36]. In undifferentiated stem cells, hypoxic conditions were induced by treatment of 10, 20, 30, 40 and 50 µM $CoCl_2$. These concentrations were decided based on the differential cytotoxic response exhibited by these cells towards $CoCl_2$ in pilot experiments. The treatment was given for two time points, 24 hours and 48 hours to mimic short term and long term hypoxic conditions respectively. Similarly, another group was maintained containing cells under hypoxic conditions which were also treated with PS at the concentration showing highest differentiation potential. The 10 µM of retinoic acid was used as a positive control in all the experiments.

Neurite outgrowth assay

The neurite outgrowth was measured as described earlier [37] with some modifications. Cellular morphology and neurite formation were observed after 48 h of treatment using an inverted microscope. Representative images were captured using a digital imaging system. Neurite length was measured using ImageJ software with the NeuronGrowth plugin. Five longest neurites from at least ten random microscopic fields per well were measured. Neurite length was defined as the

distance from the center of the cell body (soma) to the tip of the neurite. Incomplete neurites were excluded from analysis and the average neurite length was calculated.

Mitochondrial dehydrogenase activity

The mitochondrial dehydrogenase activity in SH-SY5Y cells was evaluated by 3-(4,5-dimethylthiazol-2-yl)-2,5-diphenyltetrazolium bromide (MTT) assay [34]. At the end of each treatment regime, the experiment was terminated by addition of 10 µl of MTT (5 mg mL^{-1}) in each well in dark conditions. The plates were wrapped in aluminium foil and the cultures were incubated overnight to allow for formation of the formazan crystals. The supernatant was carefully removed, and 100 µl of DMF-SDS solution was added to each well. The plates were kept at room temperature in the dark until complete dissolution of crystals and absorbance was taken at 570 nm on an ELISA microplate reader.

Preparation of cell lysate

The SH-SY5Y cells in 96 well plates were washed with calcium magnesium free phosphate buffered saline and cell suspension was prepared in 0.1% Triton-X. The cell suspension was then centrifuged at 5000 RPM and supernatant was used for further assays.

Estimation of dopamine content

The dopamine content was estimated as described earlier [38] with some modifications. The reaction mixture consisted of 100 µl buffer (pH 9.4), 25 µl of cell lysate, 25 µl of 150 mM magnesium acetate solution, 25 µl of 150 mM ammonium chloride solution and 25 µl of DMSO–water (1:1 v/v). The mixture was mixed thoroughly and allowed to stand for 15 mins at room temperature. The absorbance of the developed colour was measured at 585 nm using an ELISA microplate reader and the dopamine content was calculated from the standard curve plotted using L-Dopa.

Estimation of epinephrine content

The epinephrine content was estimated as described previously [39] with some modifications. An aliquot of 20 µL of cell lysate and 20 µL of acetone was mixed thoroughly and allowed to stand at room temperature for 10 mins. Then, 40 µL of sodium periodate solution was added and the reaction mixture was incubated for 5 mins. The final volume was adjusted to 200 µL with ethanol, mixed properly and the absorbance was measured at 490 nm using an ELISA microplate

reader and the epinephrine content was calculated from the standard curve plotted using epinephrine.

Estimation of serotonin content

The serotonin content was estimated as described earlier [40] with some modifications. Briefly, 50 µL of cell lysate was mixed with 125 µL of Ehrlich's reagent and heated in a water bath at 50 °C for 30 mins. After cooling to room temperature, 0.1 M HCl was added to obtain a final volume of 250 µL per well. The absorbance was measured at 625 nm using an ELISA microplate reader and the serotonin content was calculated from the standard curve plotted using serotonin.

Estimation of ATPase activity

The ATPase activity was determined as described previously [41] with some modifications. The reaction mixture containing 30 µl of Tris HCl Buffer (pH 7.2), 6 µl of 50 mM potassium chloride, 6 µl of 100 mM sodium chloride, 6 µl of 1mM EDTA, 6 µl of 1 mM ATP and 6 µl of cell lysate was incubated for 15 mins at 37 °C. After incubation, 30 µl of 10% TCA was added and the content was centrifuged at 5000 RPM for 10 mins. The supernatant was aliquoted and mixed with 54 µl of distilled water, 30 µl of molybdate reagent and 15 µl of ANSA reagent. The absorbance of the mixture was taken at 640 nm and the amount of inorganic phosphate (iP) liberated was determined from the standard curve plotted using sodium phosphate. The specific activity of the enzyme was then calculated in terms of per µg of iP mg protein^{-1} min^{-1}.

Estimation of AChE activity

The acetylcholinesterase activity was determined as described earlier [42] with some modifications. The reaction mixture consisted of a 2.33 mL phosphate buffer, 0.1 mL of DTNB reagent and 0.05 mL cell lysate. The mixture was allowed to equilibrate for 20 mins at 30 °C and then absorbance was read at 412 nm on the UV-VIS spectrophotometer. The substrate acetylthiocholine iodide was then added to the reaction mixture to make the total volume to 2.5 mL. The absorbance was recorded exactly after 5 minutes. The specific activity of the enzyme was calculated as per mg protein/min.

Statistical analysis

All readings were taken in triplicates and expressed as mean (± SD). The readings were analyzed by a one-sample t-test at the 5% significance level, followed by a one-way ANOVA. All tests for statistical analysis were performed in SPSS software (PASW Statistics 18)

Results:

Compositional Analysis of PS

Table 1. Biochemical analysis of PS

Contents	**Percentage**
Carbohydrate	16.69%
Uronic acids	12.66%
Sulphate	24.35%
Protein	3.77%

The compositional analysis of PS (Table 1) revealed that its major component is sulphate (24.35%), followed by carbohydrates (16.69%) and uronic acids (12.66%). On the contrary, protein was reported in minimal amounts (3.77%). The uronic acids constituted a significant portion (75.85%) of the total carbohydrate fraction as evident from their respective percentages. The high uronic acid concentration and the presence of sulphated groups suggest that PS has a significant potential bioactivity.

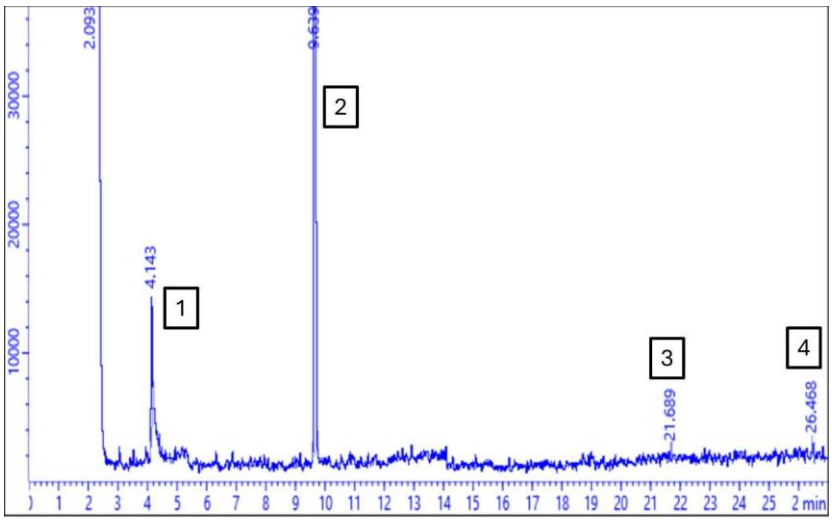

Fig. 1 GC-MS chromatogram of monosaccharides in hydrolysed PS showing peaks of (1) fucose, (2) rhamnose, (3) xylose, and (4) galactose

Table 2 Monosaccharide composition of PS (%)

Contents	**Percentage**
Fucose	19.27%
Rhamnose	37.92%
Xylose	4.76%
Galactose	5.53%

The results of GC-MS analysis of PS demonstrated the presence of four types of monosaccharides units (Table 2). Among them, rhamnose had the highest proportion (37.92%), followed by fucose (19.27%) and galactose (5.53%), while xylose had the lowest proportion (4.76%). The presence of deoxy-6-carbon sugars like rhamnose and fucose in PS is indicative of its prospective biological applications.

Differentiation potential of PS under normoxia

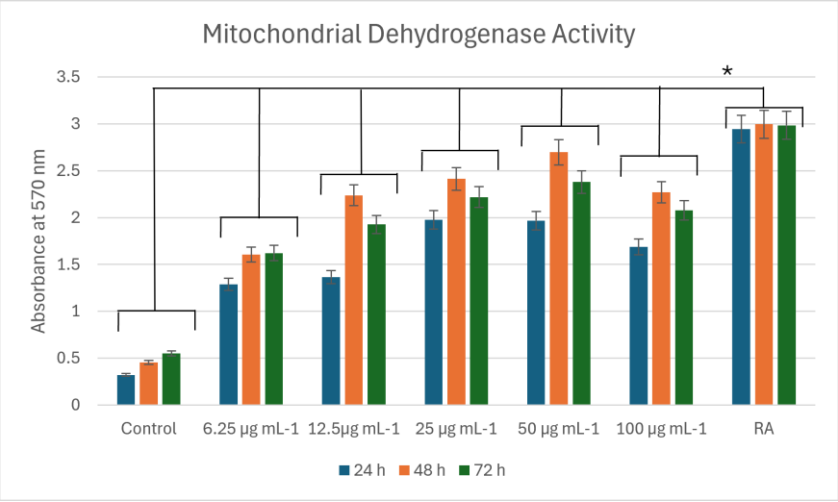

Fig. 2 Mitochondrial Dehydrogenase activity in SH-SY5Y cell line with different concentrations of PS [*significantly different from each other ($p \leq 0.05$)]

To assess the differentiation potential of PS, the mitochondrial dehydrogenase activity was evaluated as a biochemical marker for differentiation of neuronal cells. From (Figure 2) it can be observed that the mitochondrial dehydrogenase activity was lowest in the control group and highest in the retinoic acid group indicating no differentiation and complete differentiation, respectively. Following PS treatment, the activity demonstrated a concentration dependent increase from 6.25 µg mL^{-1} to 50 µg mL^{-1}, though a further increase in the concentration resulted in decreased activity. Also, across all the concentrations, the activity was always higher at 48h than 24 and 72h. Even though the highest activity was reported at 50 µg mL^{-1} test concentrations among PS treated groups, it is significantly ($p \leq 0.05$) less from the retinoic acid group.

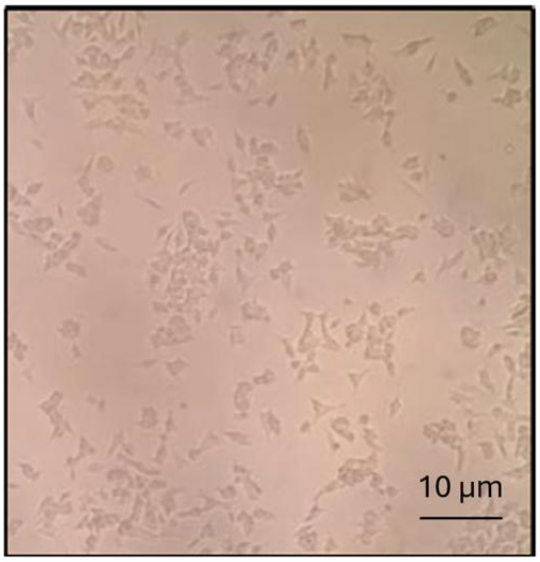

(a)

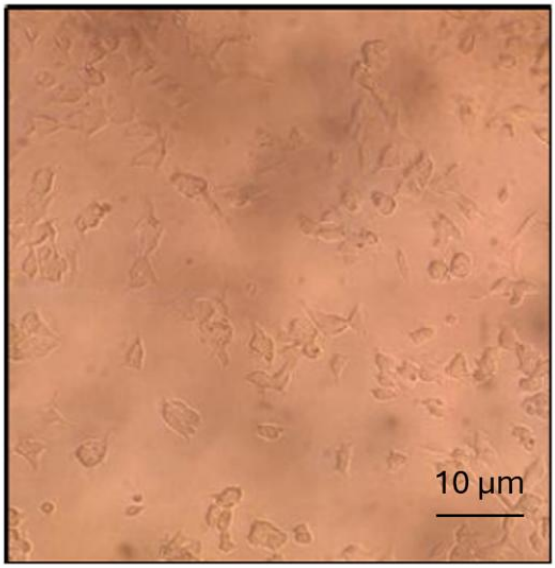

(b)

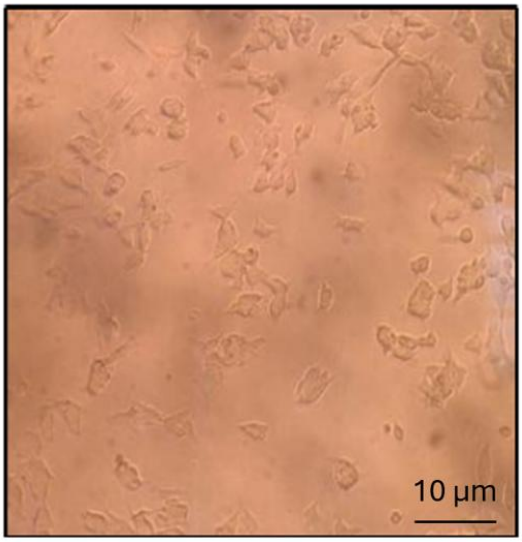

(c)

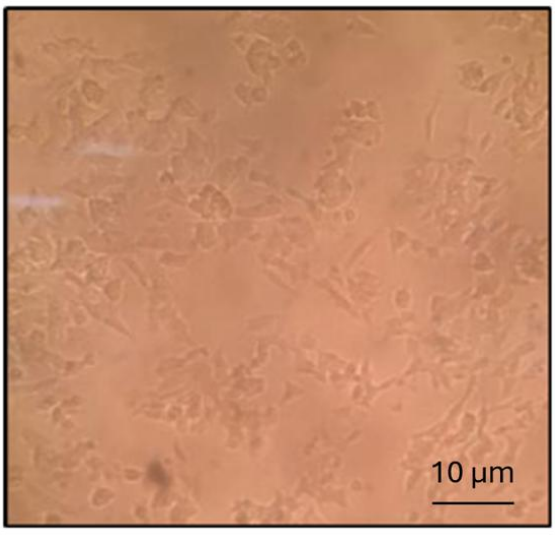

(d)

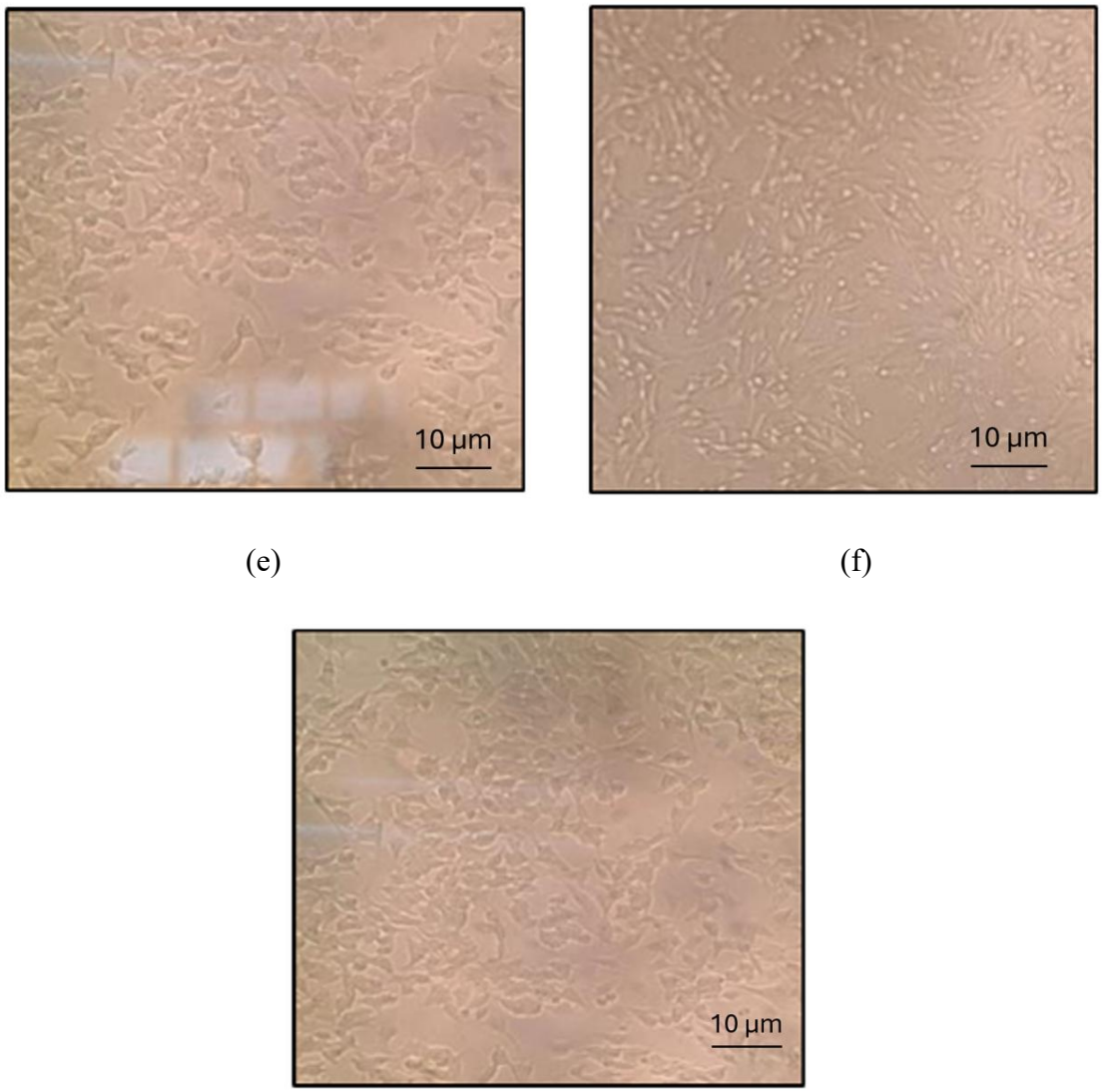

(e) (f)

(g)

Fig. 3 SH-SY5Y cells treated with various polysaccharide concentrations (a) Control, (b) 6.25 µg mL^{-1}, (c) 12.5 µg mL^{-1}, (d) 25 µg mL^{-1}, (e) 50 µg mL^{-1}, (f) 100 µg mL^{-1}, and (g) 10 µM Retinoic acid under compound microscope (40x) at 48 h

Table 3 Neurite length of SH-SY5Y cell line after treated with different concentration of PS

Group	**Neurite length (µm)**
Control	0.12 (± 0.05)
6.25 µg mL^{-1}	1.37 (± 0.03)
12.5 µg mL^{-1}	3.35 (± 0.06)
25 µg mL^{-1}	4.62 (± 0.03)
50 µg mL^{-1}	4.67 (± 0.02)
100 µg mL^{-1}	4.65 (± 0.05)
RA	4.62 (± 0.05)

The neurite outgrowth assay was also performed to assess the visual signs of differentiation. The neurite length was reported to be shortest in the control group with the average length of 0.12 (± 0.05) µm and gradually increased to the longest in 50 µg mL^{-1} with the average neurite length of 4.67 (± 0.02) µm (Table 3). The lengths reported at concentrations 25, 50, and 100 µg mL^{-1} were comparable to that reported in the retinoic acid group. By considering the results of the mitochondrial dehydrogenase assay, and neurite outgrowth evaluation, the concentration of 50 µg mL^{-1} and a time point of 48 hours were selected for all the subsequent assays as they demonstrated the highest differentiation potential.

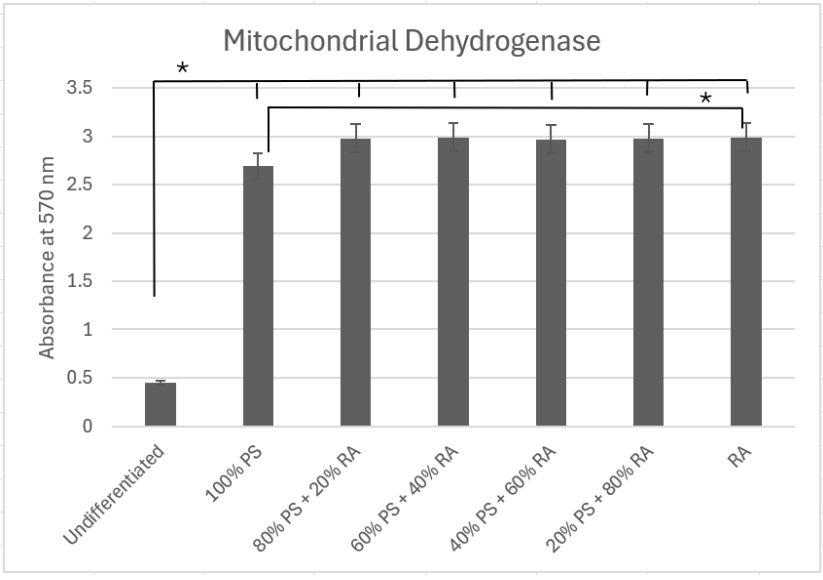

Fig. 4 Mitochondrial dehydrogenase activity in SH-SY5Y cells with various combinations of Polysaccharide (PS) and Retinoic acid (RA) [*significantly different from each other ($p \leq 0.05$)]

The RA treated cells showed highest levels of mitochondrial dehydrogenase activity, while the undifferentiated group had the lowest activity (Figure 4) indicating complete and no differentiation respectively. Compared to the undifferentiated group, treatment with 100% PS alone resulted in a substantial increase in the activity but it was significantly ($p \leq 0.05$) less than the RA treated group. The enzyme activity was found comparable in the remaining combinations of PS and RA with the RA treated group.

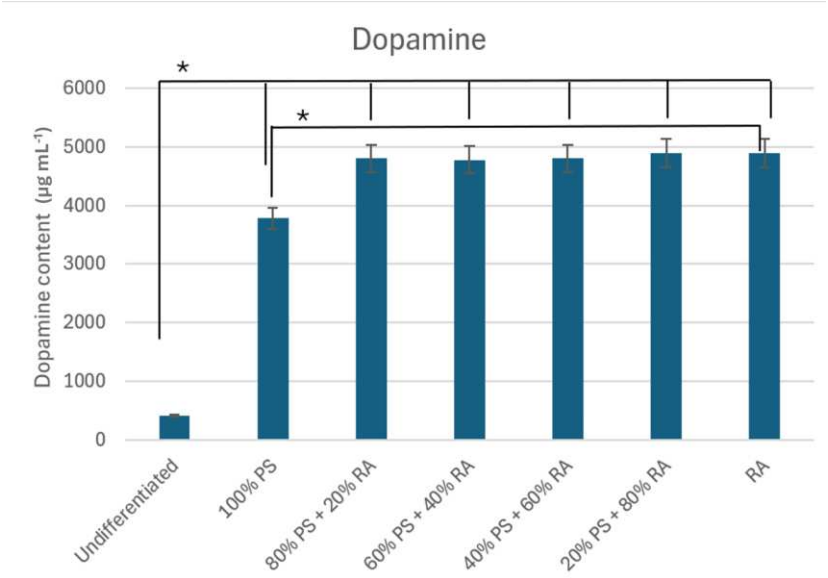

Fig. 5 Dopamine content in SH-SY5Y cells with various combinations of Polysaccharide (PS) and Retinoic acid (RA) [*significantly different from each other ($p \leq 0.05$)]

Dopamine content was reported to be minimum in undifferentiated cells, and was recorded to be maximum in the RA treated cells (Figure 5). Treatment with 100% PS significantly increased the dopamine level, however the level was still significantly lower ($p \leq 0.05$) and was not comparable with the RA treated group. The remaining concentrations showed significantly higher levels of dopamine, all of which were comparable to the RA treated group.

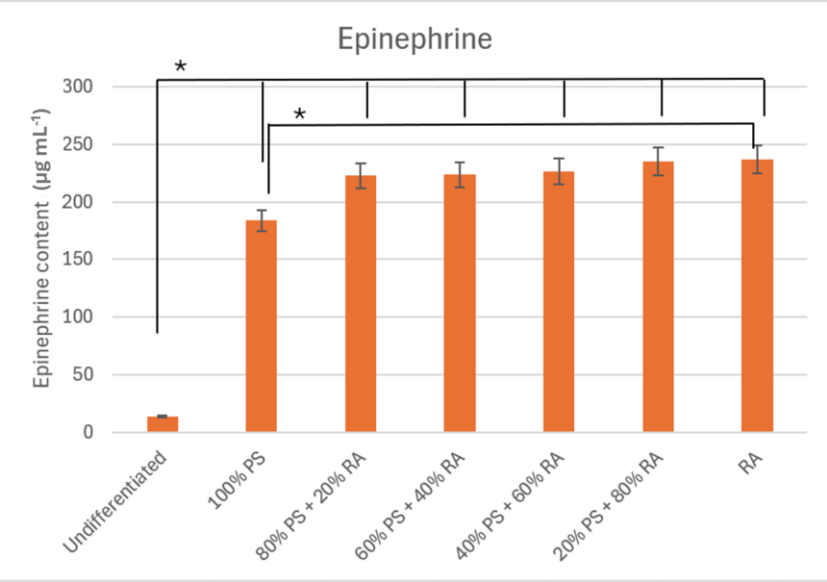

Fig. 6 Epinephrine content in SH-SY5Y cells with various combinations of Polysaccharide (PS) and Retinoic acid (RA) [*significantly different from each other ($p \leq 0.05$)]

Epinephrine level was observed to be lowest in the undifferentiated cells and highest in the RA treated group (Figure 6). Treatment with 100% PS led to a significant increase ($p \leq 0.05$) in the level of epinephrine compared to undifferentiated cells but still significantly lower ($p \leq 0.05$) compared to the RA treated group. Epinephrine concentrations in the 80% PS + 20% RA, 60% PS + 40% RA, and 40% PS + 60% RA groups were comparable to those observed in the retinoic acid control.

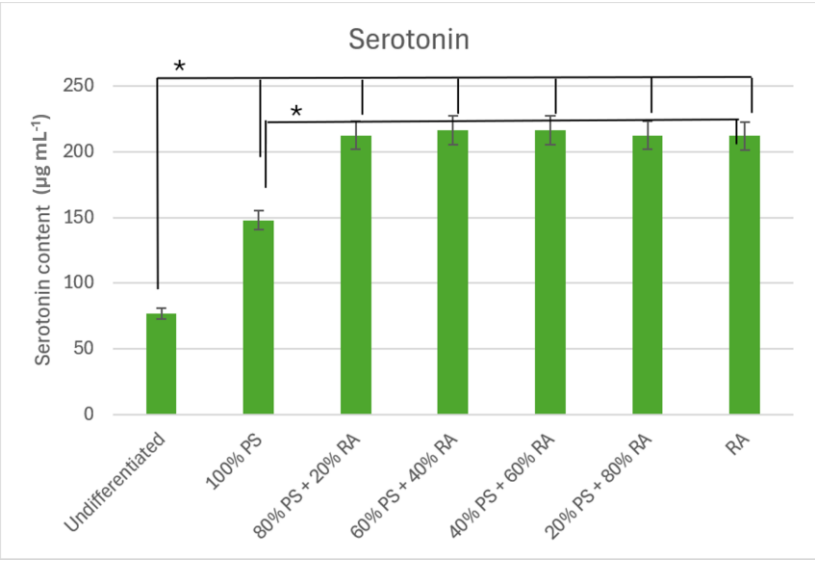

Fig. 7 Serotonin content in SH-SY5Y cells with various combinations of Polysaccharide (PS) and Retinoic acid (RA) [*significantly different from each other ($p \leq 0.05$)]

From (Figure 7) it can be seen that the serotonin levels were lowest in the undifferentiated cells and highest in the RA treated cells. Further treatment with 100% PS significantly increased ($p \leq 0.05$) the levels of serotonin compared to undifferentiated cells. However, it remained significantly lower ($p \leq 0.05$) compared to the RA treated cells. Serotonin levels comparable with the RA treated group were reported in 80% PS + 20% RA, 60% PS + 40% RA, and 40% PS + 60% RA treated groups.

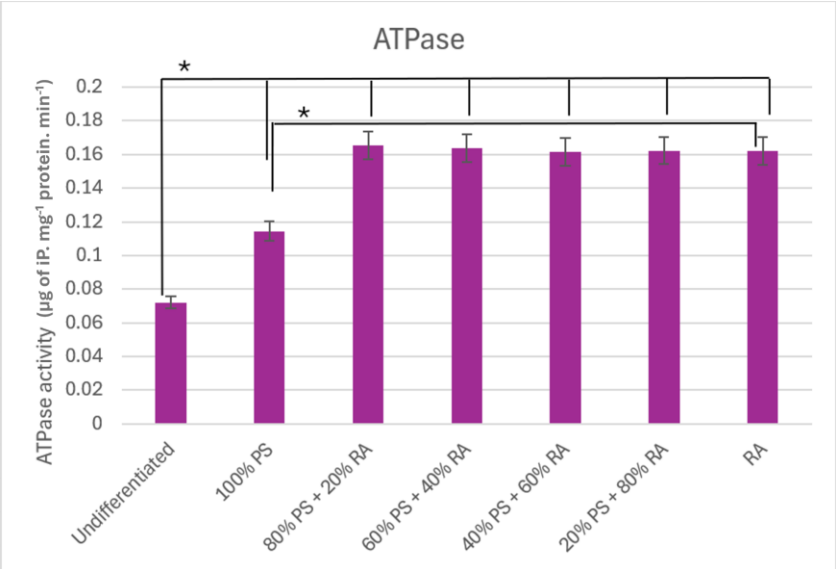

Fig. 8 ATPase activity in SH-SY5Y cells with various combinations of Polysaccharide (PS) and Retinoic acid (RA) [*significantly different from each other ($p \leq 0.05$)]

The ATPase activity was observed to be lowest in undifferentiated cells and highest in the RA treated cells (Figure 8). Treatment with 100% PS increased the enzyme activity significantly but was still significantly lower ($p \leq 0.05$) than the RA treated group. Furthermore, all the other combinations of PS and RA exhibited comparable levels of ATPase activity with the RA treated group.

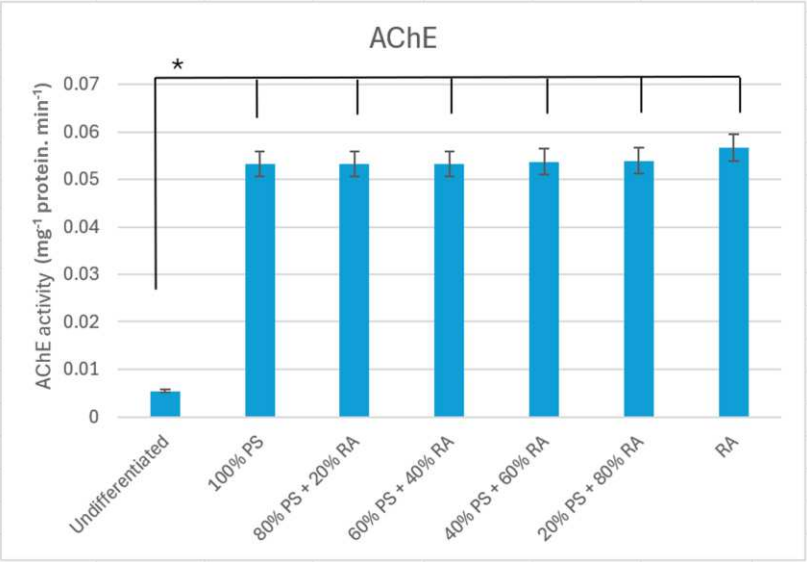

Fig. 9 AChE activity in SH-SY5Y cells with various combinations of Polysaccharide (PS) and Retinoic acid (RA) [* significantly different from each other ($p \leq 0.05$)]

The acetylcholinesterase (AChE) activity was observed to be lowest in the undifferentiated cells and highest in the RA treated cells (Figure 9). The levels of AChE activity increased substantially ($p \leq 0.05$) after treatment with different combinations of PS and RA. These increased levels in all combinations were comparable to the RA treated group, with no significant difference between the individual combinations.

Effect of PS under hypoxia

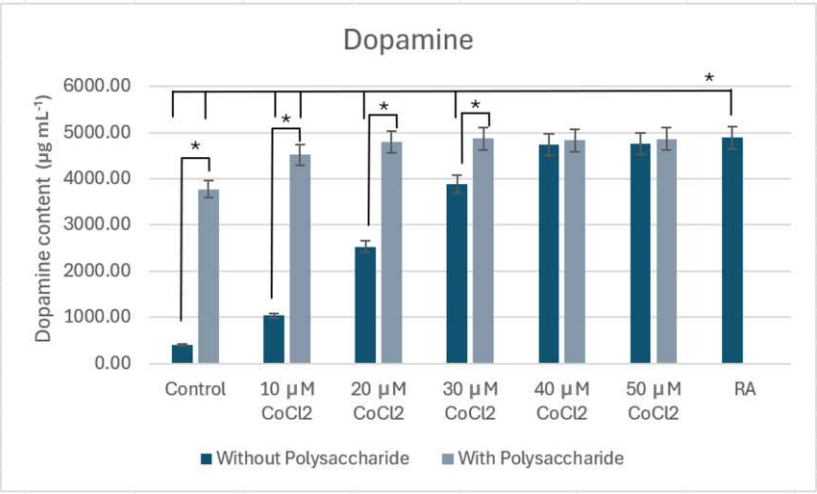

(a)

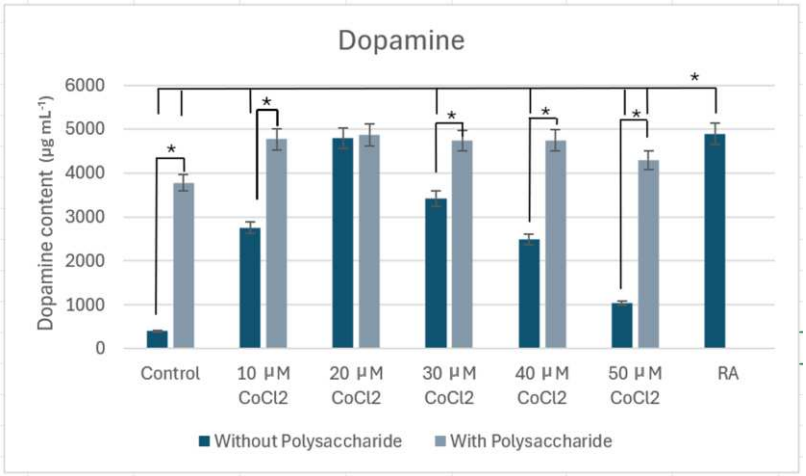

(b)

Fig. 10 Dopamine content in SH-SY5Y cells with and without polysaccharide treatment after exposure to (a) short term hypoxia (24hrs) (b) long term hypoxia (48hrs) [*significantly different from each other ($p \leq 0.05$)]

From the (Figure 10a), it can be seen that the dopamine content in the cells under short term hypoxia (24 hrs) showed gradual increase with the increasing hypoxic concentrations. Although this increase was significant ($p \leq 0.05$) in all test concentrations compared to the control set, the dopamine content in 40 and 50 µM test concentrations were only similar to that reported in the RA treated group. However, in case of PS treated cells, it can be observed that the increase in dopamine content in 20, 30, 40 and 50 µM test concentrations showed comparable results with reference to the RA treated group. This suggests that short term hypoxia at lower test concentrations results in deficient dopamine content which can be recovered to normal levels by PS treatment. In case of long-term hypoxia (48 hrs), the dopamine content increased gradually till 20 µM concentration where it was found to be comparable to the RA treated group. However, further increase in test concentrations resulted in a gradual decline in dopamine content (Figure 10b). Nevertheless, in the cells treated with PS, this variation in the dopamine levels from 10 to 50 µM concentrations got neutralized and the content was comparable to the RA treated group.

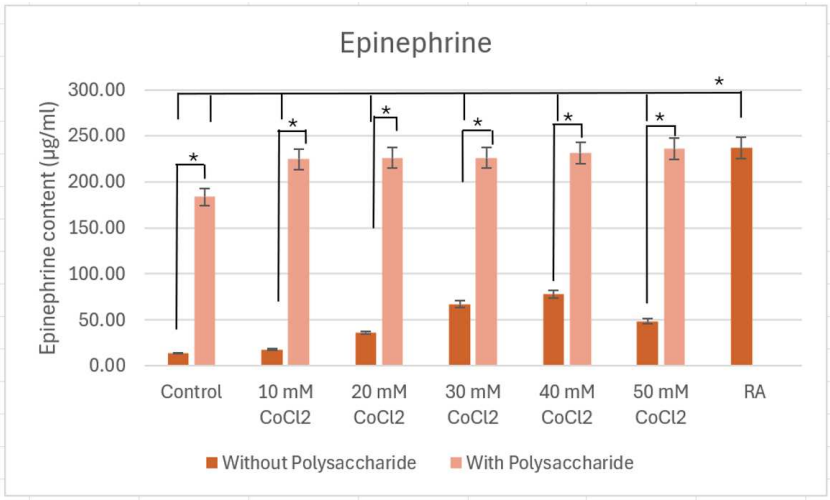

(a)

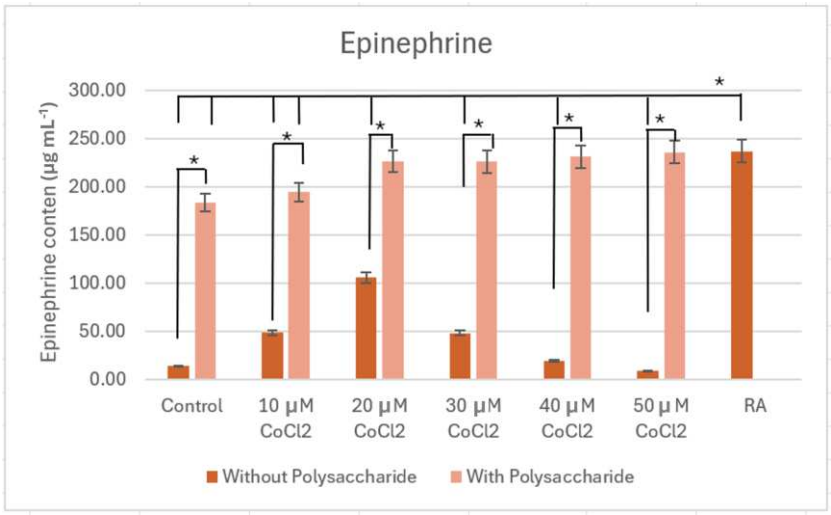

(b)

Fig. 11 Epinephrine content in SH-SY5Y cells with and without polysaccharide treatment, after exposure to (a) short term hypoxia (24hrs) (b) long term hypoxia (48hrs) [*significantly different from each other ($p \leq 0.05$)]

The epinephrine levels are observed to be minimal in the control group in short term (24h) hypoxia (Figure 11a). The hypoxic concentrations, 10, 20, 30 and 40 µM showed gradual significant ($p \leq 0.05$) increase in the epinephrine levels compared to the control set; however further increase in the concentration led to a decline. Although these elevated levels were higher than those in the control group, they remained significantly ($p \leq 0.0$) lower than in the RA-treated group. The PS-treated groups exhibited epinephrine levels comparable to the RA-treated set, showing no significant differences among individual concentrations. Under long term hypoxia (48h), epinephrine levels in non-treated cells peaked at 20 µM before declining to minimal levels (Figure 11b), though the highest epinephrine level at 20 µM remained significantly ($p \leq 0.05$) low when

compared to the RA- treated group. In the PS treated sets, the epinephrine levels exhibited insignificant differences in 20, 30, 40 and 50 µM concentrations, showing equivalent levels compared to the RA treated set.

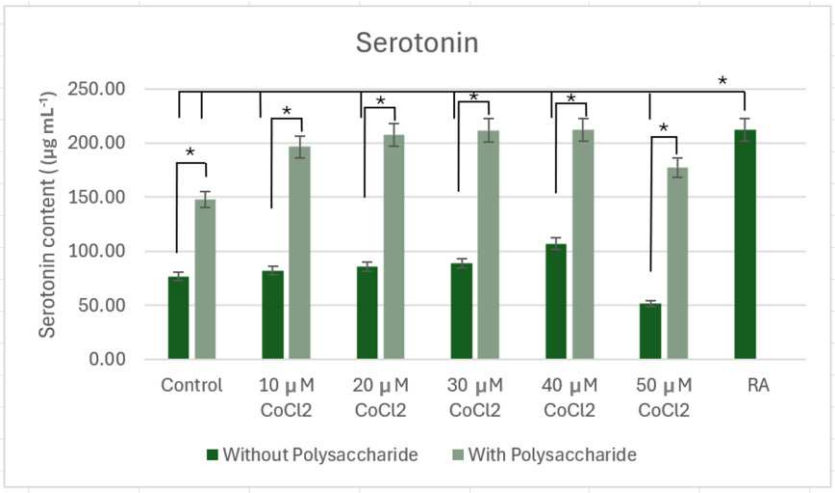

(a)

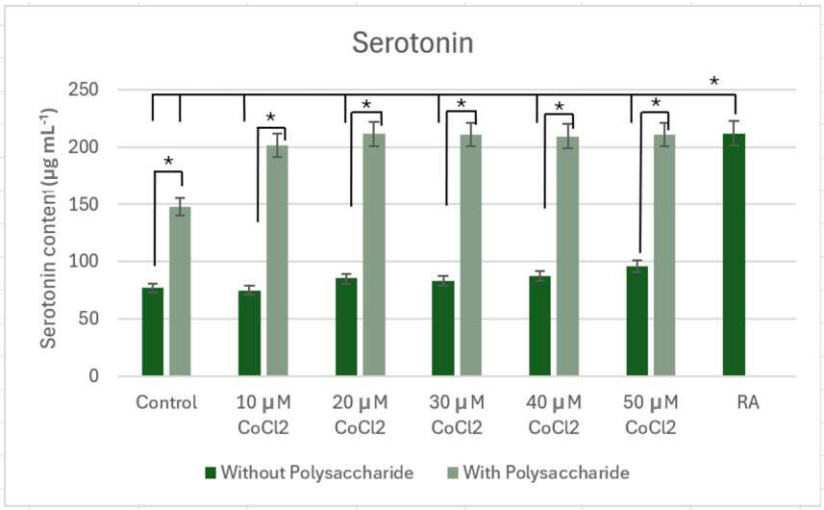

(b)

Fig. 12 Serotonin content in SH-SY5Y cells with and without polysaccharide treatment, after exposure to (a) short term hypoxia (24hrs) (b) long term hypoxia (48hrs) [*significantly different from each other ($p \leq 0.05$)]

In short-term hypoxia (24 h), serotonin levels in untreated cells increased gradually compared to the control set, peaking at the concentration of 40 µM, before dropping significantly ($p \leq 0.05$) (Figure 12a). However, this peak level was still significantly ($p \leq 0.05$) lower than the RA-treated group. In contrast, the cells treated with PS exhibited higher levels of serotonin across control and

the remaining concentrations, with that in 10, 20, 30 and 40 µM showing levels comparable to the RA-treated cells. In long-term hypoxia (48 h), all the concentrations without PS treatment demonstrated significantly lower serotonin levels compared to the RA-treated group (Figure 12b). In PS treated groups, the serotonin levels recovered and remained comparable to the RA treated group with no significant ($p \leq 0.05$) difference among individual concentrations.

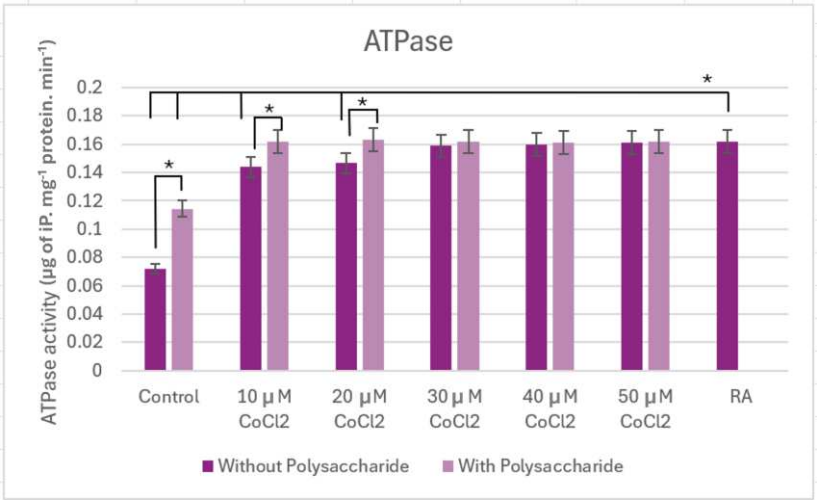

(a)

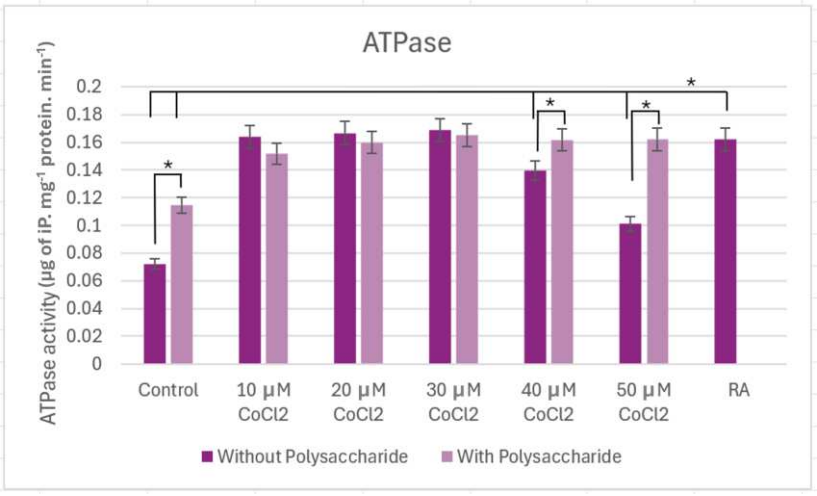

(b)

Fig. 13 ATPase activity in SH-SY5Y cells with and without polysaccharide treatment, after exposure to (a) short term hypoxia (24hrs) (b) long term hypoxia (48hrs) [*significantly different from each other ($p \leq 0.05$)]

Under short-term hypoxia (24 h) in untreated cells, the ATPase activity was lowest in the control group and gradually increased with the increasing hypoxic concentration (Figure 13a). This increased enzyme activity was nearly equivalent to the RA-treated group at concentrations 30, 40

and 50 µM. In the PS treated cells, the activity remained lowest in the control set; however, even at the lowest hypoxic concentration of 10 µM, ATPase activity increased significantly and remained comparable to RA-treated cells. Under long-term hypoxia (48 h) in untreated cells, the ATPase activity remained minimal in the control group (Figure 13b). Activity increased substantially at lower concentrations (10, 20 and 30 µM) reaching levels equivalent to the RA-treated cells, before gradually decreasing at 40 and 50 µM. Although the PS treated set showed lower ATPase activity in the control set, activity increased across all the hypoxic concentrations significantly ($p \leq 0.05$) and remained comparable to the RA-treated groups.

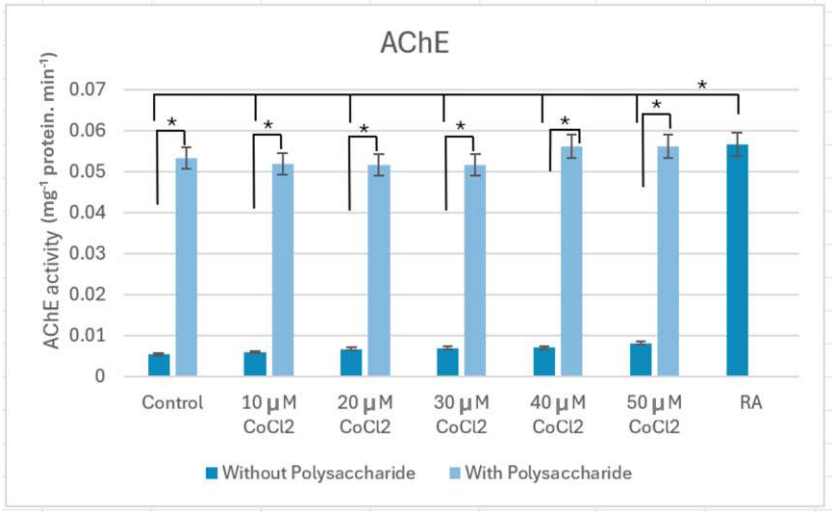

(a)

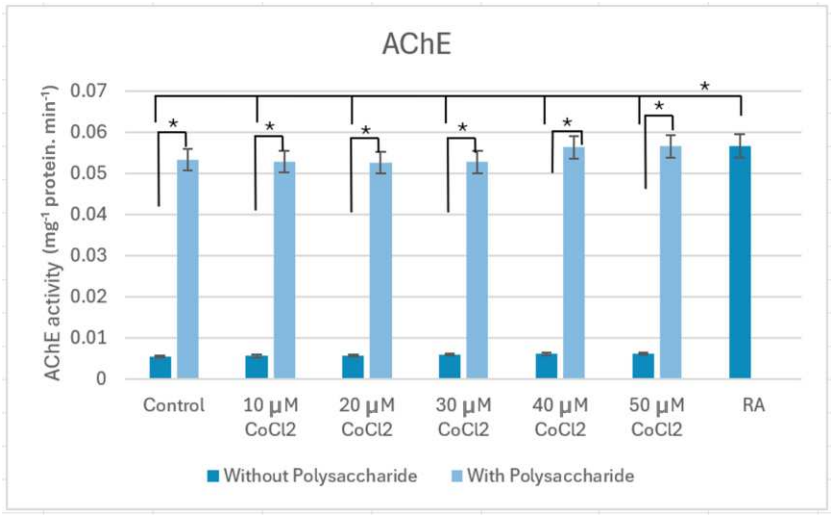

(b)

Fig. 14 AChE activity in SH-SY5Y cells with and without polysaccharide treatment, after exposure to (a) short term hypoxia (24hrs) (b) long term hypoxia (48hrs) [*significantly different from each other ($p \leq 0.05$)]

Under short term hypoxia (24hrs) in untreated cells, the acetylcholinesterase (AChE) activity was recorded to be minimal in the control group and differs insignificantly across all the hypoxic concentrations (Figure 14a). These levels were also significantly lower than the RA treated cells. However, in the PS-treated cells, AChE activity increased significantly even at the lowest hypoxic concentration (10 µM) and remained consistently comparable to that of RA-treated cells. Under long-term hypoxia (48hrs) in untreated cells, the activity remained minimal, similar to the short-term conditions (Figure 14b). PS treated cells also demonstrated a similar trend, where AChE activity increased at the lowest hypoxic concentration and remained on par with RA treated cells across all the concentrations.

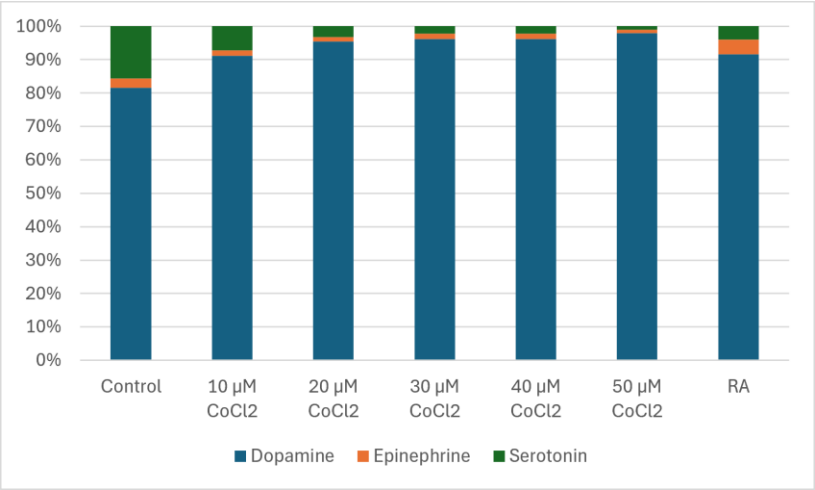

(a)

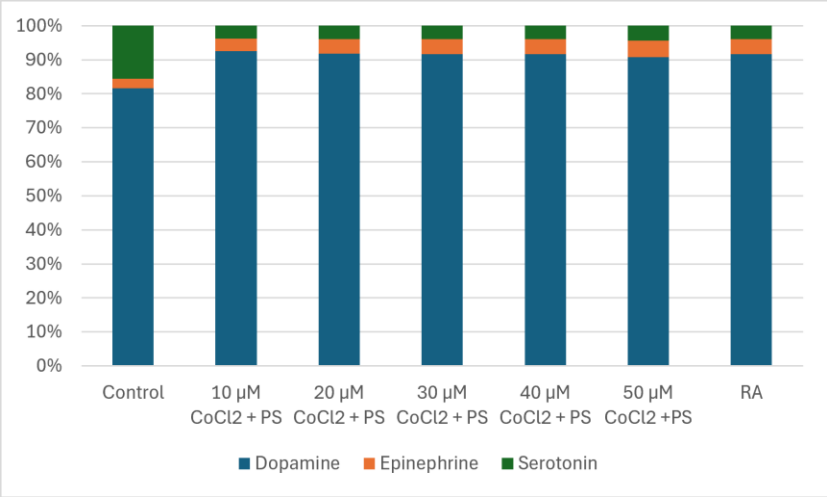

(b)

Fig. 15 Relative percentage of neurotransmitters in sh-sy5y cells under short-term (24 h) hypoxic conditions (a) without polysaccharide treatment (b) with polysaccharide treatment

Under short term hypoxia (24h) relative neurotransmitter percentage of untreated cells demonstrated an overall imbalance compared to the control as well as RA treated group (Figure 15a). At 10 µM concentration, the relative proportion of dopamine was comparable to the RA group; though lower epinephrine and higher serotonin percentages were reported. However, further increase in the hypoxic concentration led to elevated dopamine levels and subsequently reduced serotonin as well as epinephrine levels. In contrast, the relative neurotransmitter percentage in PS treated cells remained comparatively stable (Figure 15b) with dopamine, serotonin and epinephrine levels remaining comparable to the RA-treated group across all hypoxic concentrations.

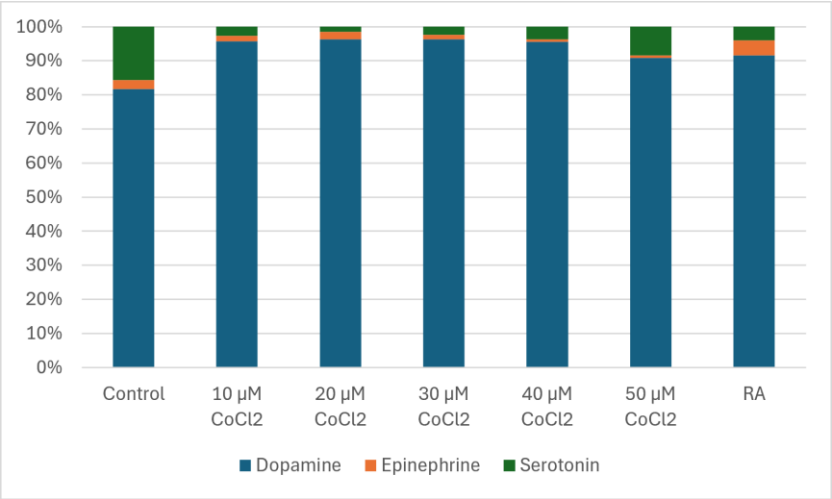

(a)

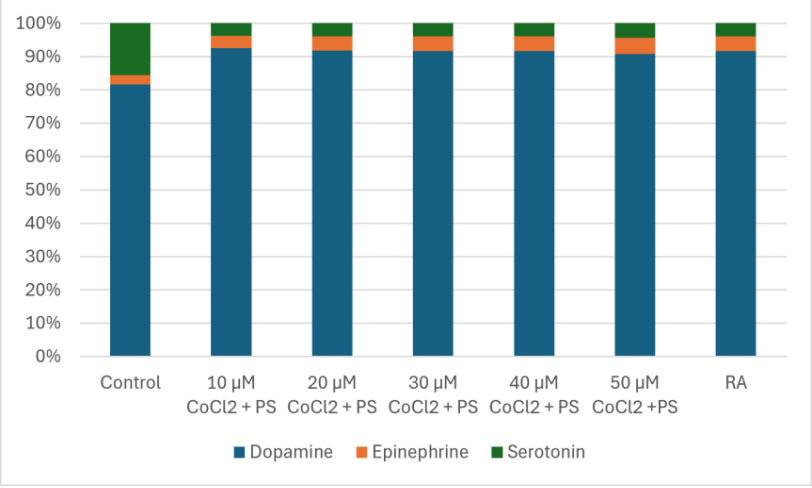

(b)

Fig. 16 Relative percentage of neurotransmitters in sh-sy5y cells under long-term (48 h) hypoxic conditions (a) without polysaccharide treatment (b) with polysaccharide treatment

Under long term hypoxia (48h), relative neurotransmitter percentage analysis of untreated cells demonstrated variable neurotransmitter levels in different hypoxic concentrations (Figure 16a). Levels of dopamine remained elevated in 10, 20, 30 and 40 μM hypoxic concentrations, with subsequently reduced serotonin and epinephrine levels. Notably, at the 50 μM concentration the percentage of dopamine remained comparable to the RA treated group, with reduced epinephrine levels and higher serotonin percentage. In contrast, the relative neurotransmitter percentage in PS treated cells remained comparatively stable (Figure 16b) with dopamine, serotonin and epinephrine levels remaining comparable to the RA treated group.

Discussions

Since their emergence on Earth approximately 1.5 billion years ago, algae have played a significant role in the carbon cycle and have also served as a source of nutraceuticals for various indigenous cultures globally [22]. Among the different nutraceutical elements present in algae, algal polysaccharides have recently attracted considerable attention as potential organic drugs due to their diverse bioactivities. Polysaccharides, including carrageenan, agar, agarose, and porphyran from red algae; fucoidan, laminarin, and alginate from brown algae; and ulvan from green algae, exhibit distinct chemical structures influenced by their monosaccharide composition, degree of sulfation, and types of glycosidic linkages [43]. These structural characteristics allow them to interact with cell membranes and their receptors, which is directly related to their bioactivity. Consequently, these polysaccharides have shown encouraging therapeutic benefits in both *in vivo* and *in vitro* experiments [44]. Several polysaccharides derived from marine microalgae have demonstrated neuroprotective effects across experimental models of neurodegeneration [27]. The significance of algal polysaccharides in terms of their extraction, purification, and their applications in a variety of industries has been well explained by the scientific community. Nevertheless, these algal polysaccharides need thorough research despite all of their captivating characteristics and potential in the medical field [45]. Therefore, the present study was undertaken to assess the potential of crude polysaccharide obtained from indigenous marine microalgae to induce neuronal stem cell differentiation and to mitigate hypoxia induced neuronal damage *in vitro*.

The biochemical analysis of a polysaccharide derived from *Phormidium persicinum* revealed sulphate as a major component followed by carbohydrates, uronic acids and protein (Table 1). The relatively high sulphate content reported in the polysaccharide sample, may be accounted for its

biological activity as sulphated polysaccharides have revealed their potential in management of Parkinson's disease through anti-amyloidogenic effects in earlier study [46]. Additionally, it has been claimed that uronic acids, particularly those found in glycosaminoglycans like hyaluronic acid and glucuronic acid, are important for neural differentiation because they provide structural and chemical signals in the extracellular matrix that direct the behaviour of neural stem cells [47]. Monosaccharide analysis of PS revealed rhamnose as the major component, followed by fucose, galactose, and xylose (Table 2). Rhamnose-containing polysaccharides have been reported to exhibit bioactive properties of neuroprotection and neural differentiation in earlier reports [48, 49]. Similarly, galactose and xylose containing polysaccharides have also been associated with neuroprotective effects, neural differentiation and are known to promote neuronal growth [50, 51]. A recent study on L-fucose reported that it played an important role in neuromodulation and neuronal signalling [52]. These findings suggest that the components of *Phormidium persicinum* polysaccharide may contribute to its neuroprotective and differentiation-promoting properties.

Neuronal differentiation is marked by metabolic reprogramming, characterised by a shift from aerobic glycolysis to oxidative phosphorylation [53]. Therefore, mitochondrial dehydrogenase activity is the key biochemical indicator of neuronal differentiation. The activity of mitochondrial dehydrogenase was therefore recorded in SH-SY5Y cells treated across various concentrations of polysaccharide with retinoic acid serving as a positive control (Figure 2). The highest activity was recorded at 50 μg mL^{-1} but remained significantly lower than the retinoic acid group. However, neurite length analysis revealed comparable morphological differentiation at concentrations of 25, 50 and 100 μg mL^{-1} when compared to the retinoic acid group (Table 3). Therefore, it can be noted that even while neural cells exhibit complete neurite formation under these circumstances, mitochondrial dehydrogenase activity was not at its optimal level. This suggests that despite complete visible differentiation of neuronal cells, the state of differentiation did not corroborate at biochemical level. In order to ascertain the ideal circumstances for differentiation at both the visual and biochemical levels, PS and retinoic acid were utilised in various combinations in subsequent investigations and biochemical parameters like activities of mitochondrial dehydrogenase, acetylcholinesterase, ATPase along with levels of dopamine, epinephrine, and serotonin were evaluated. It was observed that the treatment with polysaccharide alone significantly increased enzyme activity and neurotransmitter levels; however, these levels remained significantly lower than those observed in the retinoic acid group (Figures 4-9). Nevertheless, treatment with PS and retinoic acid in all test combinations resulted in comparable levels of enzyme activity and neurotransmitters to those of the RA group, indicating biochemical differentiation comparable to

the RA group. This indicates the synergistic effect of PS and retinoic acid may be responsible for the complete neuronal differentiation. The uronic acids and sulphate groups present in PS may be accounted for this synergistic effect. Uronic acids have been reported to bind with CD44 receptors on neuronal stem cells and trigger the shift of metabolism from proliferation to differentiation of these cells [47]. Additionally, polysaccharides with specific sulphation patterns have been documented to form wobble motifs that induce differentiation of neural stem cells by modulating ERK/MAPK signaling pathway [54]. Though similar induction of neural stem cell differentiation was reported in earlier studies synergistically with retinoic acid [55] this is the first study to report it with algal polysaccharide.

Hypoxia has been associated with pathogenesis in neurodegenerative diseases including Parkinson's and Alzheimer's disease, through processes involving mitochondrial dysfunction and oxidative stress [56, 57]. Therefore, in the current study, hypoxia was used as an experimental stress condition to investigate the neuroprotective potential of PS. Previous studies have reported alteration in dopamine levels depending on the duration and severity of hypoxia [58]. In a recent study on SH-SY5Y cells, hypoxia induced activation of HIF-1∝ increased expression of tyrosine hydroxylase and dopamine transporter through ERRγ, indicating that hypoxia can influence dopamine synthesis and transport [59]. In the current study, under short term (24hrs) hypoxia, untreated cells showed concentration dependent increase of dopamine levels. PS treated cells showed dopamine levels comparable to RA at 40 and 50 μM hypoxic concentrations (Figure 10a). Under long term (48hrs) hypoxia, untreated cells showed dopamine levels comparable to RA-treated cells only at 20μM concentration; however, treatment with PS attenuated these variations, maintaining dopamine levels comparable to the RA-treated group (Figure 10b). Hypoxia has been reported to affect the expression of phenylethanolamine N-methyltransferase (PNMT), an enzyme implicated for epinephrine biosynthesis in PC12 cells [60]. In the present study, untreated cells under short term (24hrs) hypoxia, the epinephrine levels gradually increased till 40μM concentration, while remaining significantly lower than the RA group (Figure 11a). In PS-treated cells, the epinephrine levels increased substantially and were comparable with the RA-treated set across all hypoxic concentrations. Under long term (48hrs) hypoxia, the epinephrine levels in untreated cells peaked at 20 μM but stayed significantly lower than the RA-treated group (Figure 11b). In PS-treated cells these variations remained attenuated, with epinephrine levels remaining comparable with the RA-treated group across all hypoxic concentrations. Hypoxia has been reported to impair tryptophan hydroxylase (TPH), the enzyme involved in serotonin synthesis, resulting in reduced serotonergic functions [61]. Furthermore, these alterations in TPH and

serotonin content have been reported to be partially restored by antioxidant treatment [62]. In the present study, untreated cells under short term (24hrs) hypoxia, serotonin levels increased gradually till 40 μM, while remaining significantly lower than the RA-treated group (Figure 12a). PS-treated cells exhibited higher levels of serotonin with concentrations 10, 20, 30 and 40 μM showing comparable values to the RA-treated group. Under long term (48hrs) hypoxia, untreated cells exhibited significantly lower levels of serotonin across all the concentrations (Figure 12b). However, PS-treated cells exhibited comparable levels with the RA-treated group across the concentrations. Hypoxia has been known to disrupt ATPase activity, which plays an important role in maintaining cellular homeostasis. Studies in neuronal cells have demonstrated that hypoxic conditions can suppress Na^+/K^+-ATPase activity [63]. In present study, under short-term hypoxia, the ATPase activity in untreated cells gradually increases at higher concentrations (Figure 13a). The increase may represent an adaptive response to moderate hypoxic stress, potentially helping to maintain cellular ionic homeostasis. A similar increase in Na^+/K^+-ATPase activity following hypoxic stress has been reported in the brain, proposed to play a compensatory role in maintaining Na^+ and K^+ homeostasis [64]. In contrast, PS treatment increased ATPase activity to levels comparable to those in RA-treated cells, even at the lower hypoxic concentrations. Under long-term hypoxia, the untreated cells exhibited decreasing ATPase activity as the concentration increased (Figure 13b). This decrease may indicate that the initial adaptive response was progressively compromised under prolonged hypoxic stress [65]. The PS treatment maintained ATPase activity at levels comparable to those of the RA-treated cells across the hypoxic concentrations, suggesting that PS may have helped preserve ATP-dependent cellular functions under prolonged hypoxic stress. AChE activity has been reported to be responsive to oxidative stress in SH-SY5Y cells, as H_2O_2 exposure was shown to significantly alter AChE activity [66]. Furthermore, AChE activity has also been reported to be substantially higher in differentiated than in undifferentiated SH-SY5Y cells, suggesting an association between increased AChE activity and neuronal differentiation [67]. In the present study, under short-term hypoxia the AChE activity in untreated cells remained minimal across all the concentrations with no significant difference (Figure 14a). PS treatment significantly increased the AChE activity comparable to those of RA-treated cells. Similar results were observed in long-term hypoxia (Figure 14b). This elevation in the AChE activity following PS treatment, together with the results obtained from the neurite growth assay and mitochondrial dehydrogenase activity, supports the potential of PS to promote neuronal differentiation. The study on the polysaccharide obtained from seaweed *Sargassum dentifolium* have been reported to demonstrate anti-hypoxic effects by downregulating hypoxia

associated micro-RNAs that stabilizes HIF [68]. The results of the current study reinforce these findings at biochemical levels.

Neurotransmitters play an important role in regulating neuronal communication and diverse physiological processes including motor, cognitive, involuntary physiological response and emotional regulation. Disruption of neurotransmitter synthesis or homeostasis impairs normal neuronal functioning; moreover, it has also been linked to various neuronal disorders [69, 70]. For instance, degeneration of dopaminergic neurons is associated with Parkinson's disease, while lower levels of dopamine is linked to ADHD with low or dysregulated dopamine availability affecting focus and motivation. Lower levels of serotonin is linked with anxiety and depression [71, 72]. In the present study, a relative analysis of neurotransmitter profile under short-term hypoxia revealed that the untreated cells demonstrated an overall imbalance of dopamine, serotonin and epinephrine at higher hypoxic conditions (Figure 15a). In contrast, PS-treatment maintained a stable neurotransmitter profile (Figure 15b). Similar results were obtained in long-term hypoxia, wherein the untreated cells exhibited alteration in the neurotransmitter levels, with increasing levels of dopamine and subsequently reduced levels of serotonin and epinephrine (Figure 16a). This imbalance was attenuated by PS treatment (Figure 16b). These results are in line with the earlier study which reports the protective effect of sulphated polysaccharide against dopaminergic neurodegeneration by modulating PI3K/Akt pathway [72]. Furthermore, it was documented that L-fucose, which is present in PS, ameliorates chronic social defeat stress-induced depressive-like behaviors in experimental animal models [73]. These results, therefore, underscore the prospective importance of PS to mitigate neurodegenerative effects of hypoxia.

Conclusion

The crude polysaccharide extracted from indigenous marine microalga *Phormidium persicinum* (Reinke) Gom. demonstrated promising neurodifferentiation activity when tested *in vitro* on human neuronal stem (SH-SY5Y) cells. The polysaccharide is reported to contain a mixture of biologically active components like sulphate, uronic acids, proteins, etc. and a blend of unique monosaccharides which are documented to have excellent neuroprotective activity. The polysaccharide induced complete neuronal stem cell differentiation at a concentration of 50 µg mL^{-1} when treated with 100 µM of retinoic acid in the ratio 80:20. This is the first reported study, till date, wherein the algal polysaccharide was found to be effective for inducing neurodifferentiation when cotreated with retinoic acid. Furthermore, the treatment of

polysaccharide in the same combination ameliorated the biochemical disruptions in SH-SY5Y caused by chemical hypoxia. These results highlight the need for further research to develop the purification strategy for pinpointing specific components in polysaccharide responsible for its bioactivity.

Data availability

The datasets generated during and/or analysed during the current study will be made available from the corresponding author on reasonable request

References

1. Kahroba, H., Ramezani, B., Maadi, H., Sadeghi, M. R., Jaberie, H., & Ramezani, F. (2021). The role of Nrf2 in neural stem/progenitors cells: From maintaining stemness and self-renewal to promoting differentiation capability and facilitating therapeutic application in neurodegenerative disease. *Ageing Research Reviews*, *65*, 101211. https://doi.org/10.1016/j.arr.2020.101211
2. Yaribeygi, H., Panahi, Y., Javadi, B., & Sahebkar, A. (2018). The Underlying Role of Oxidative Stress in Neurodegeneration: A Mechanistic Review. *CNS & Neurological Disorders - Drug Targets*, *17*(3), 207–215. https://doi.org/10.2174/1871527317666180425122557
3. Zhou, J., Jangili, P., Son, S., Ji, M. S., Won, M., & Kim, J. S. (2020). Fluorescent Diagnostic Probes in Neurodegenerative Diseases. *Advanced Materials*, *32*(51), 2001945. https://doi.org/10.1002/adma.202001945
4. C. Correia, S., Carvalho, C., Cardoso, S., X. Santos, R., I. Plácido, A., Candeias, E., … I. Moreira, P. (2013). Defective HIF Signaling Pathway and Brain Response to Hypoxia in Neurodegenerative Diseases: Not an "Iffy" Question! *Current Pharmaceutical Design*, *19*(38), 6809–6822. https://doi.org/10.2174/1381612811319380013
5. Daulatzai, M. A. (2013). Death by a Thousand Cuts in Alzheimer's Disease: Hypoxia—The Prodrome. *Neurotoxicity Research*, *24*(2), 216–243. https://doi.org/10.1007/s12640-013-9379-2

6. Nalivaeva, N. N., & Rybnikova, E. A. (2019). Editorial: Brain Hypoxia and Ischemia: New Insights Into Neurodegeneration and Neuroprotection. *Frontiers in Neuroscience*, *13*, 770. https://doi.org/10.3389/fnins.2019.00770
7. Li, X., Huang, L., Lan, J., Feng, X., Li, P., Wu, L., & Peng, Y. (2021). Molecular mechanisms of mitophagy and its roles in neurodegenerative diseases. *Pharmacological Research*, *163*, 105240. https://doi.org/10.1016/j.phrs.2020.105240
8. Pasteuning-Vuhman, S., De Jongh, R., Timmers, A., & Pasterkamp, R. J. (2021). Towards Advanced iPSC-based Drug Development for Neurodegenerative Disease. *Trends in Molecular Medicine*, *27*(3), 263–279. https://doi.org/10.1016/j.molmed.2020.09.013
9. McCrary, M. R., Jesson, K., Wei, Z. Z., Logun, M., Lenear, C., Tan, S., … Wei, L. (2020). Cortical Transplantation of Brain-Mimetic Glycosaminoglycan Scaffolds and Neural Progenitor Cells Promotes Vascular Regeneration and Functional Recovery after Ischemic Stroke in Mice. *Advanced Healthcare Materials*, *9*(5), 1900285. https://doi.org/10.1002/adhm.201900285
10. Barker, R. A., Götz, M., & Parmar, M. (2018). New approaches for brain repair—from rescue to reprogramming. *Nature*, *557*(7705), 329–334. https://doi.org/10.1038/s41586-018-0087-1
11. Zhang, B., Yan, W., Zhu, Y., Yang, W., Le, W., Chen, B., … Cheng, L. (2018). Nanomaterials in Neural-Stem-Cell-Mediated Regenerative Medicine: Imaging and Treatment of Neurological Diseases. *Advanced Materials*, *30*(17), 1705694. https://doi.org/10.1002/adma.201705694
12. Andreotti, J. P., Silva, W. N., Costa, A. C., Picoli, C. C., Bitencourt, F. C. O., Coimbra-Campos, L. M. C., … Birbrair, A. (2019). Neural stem cell niche heterogeneity. *Seminars in Cell & Developmental Biology*, *95*, 42–53. https://doi.org/10.1016/j.semcdb.2019.01.005
13. Reynolds, B. A., & Weiss, S. (1992). Generation of Neurons and Astrocytes from Isolated Cells of the Adult Mammalian Central Nervous System. *Science*, *255*(5052), 1707–1710. https://doi.org/10.1126/science.1553558
14. Benner, E. J., Luciano, D., Jo, R., Abdi, K., Paez-Gonzalez, P., Sheng, H., … Kuo, C. T. (2013). Protective astrogenesis from the SVZ niche after injury is controlled by Notch modulator Thbs4. *Nature*, *497*(7449), 369–373. https://doi.org/10.1038/nature12069
15. Pous, L., Deshpande, S. S., Nath, S., Mezey, S., Malik, S. C., Schildge, S., … Schachtrup, C. (2020). Fibrinogen induces neural stem cell differentiation into astrocytes in the

subventricular zone via BMP signaling. *Nature Communications*, *11*(1), 630. https://doi.org/10.1038/s41467-020-14466-y

16. Tejeda, G., Ciciriello, A. J., & Dumont, C. M. (2022). Biomaterial Strategies to Bolster Neural Stem Cell-Mediated Repair of the Central Nervous System. *Cells Tissues Organs*, *211*(6), 655–669. https://doi.org/10.1159/000515351
17. Bruggeman, K. F., Moriarty, N., Dowd, E., Nisbet, D. R., & Parish, C. L. (2019). Harnessing stem cells and biomaterials to promote neural repair. *British Journal of Pharmacology*, *176*(3), 355–368. https://doi.org/10.1111/bph.14545
18. Bellenchi, G. C., Volpicelli, F., Piscopo, V., Perrone-Capano, C., & Di Porzio, U. (2013). Adult neural stem cells: an endogenous tool to repair brain injury? *Journal of Neurochemistry*, *124*(2), 159–167. https://doi.org/10.1111/jnc.12084
19. Yang, Y., Fan, Y., Zhang, H., Zhang, Q., Zhao, Y., Xiao, Z., … Dai, J. (2021). Small molecules combined with collagen hydrogel direct neurogenesis and migration of neural stem cells after spinal cord injury. *Biomaterials*, *269*, 120479. https://doi.org/10.1016/j.biomaterials.2020.120479
20. Lee, H.-R., Farhanullah, Lee, J., Jajoo, R., Kong, S.-Y., Shin, J.-Y., … Kim, H.-J. (2016). Discovery of a Small Molecule that Enhances Astrocytogenesis by Activation of STAT3, SMAD1/5/8, and ERK1/2 via Induction of Cytokines in Neural Stem Cells. *ACS Chemical Neuroscience*, *7*(1), 90–99. https://doi.org/10.1021/acschemneuro.5b00243
21. Zhu, Y., Huang, R., Wu, Z., Song, S., Cheng, L., & Zhu, R. (2021). Deep learning-based predictive identification of neural stem cell differentiation. *Nature Communications*, *12*(1), 2614. https://doi.org/10.1038/s41467-021-22758-0
22. Joshi, D., Oza, D. H., & Vyas, P. (2026). Unlocking the Potential of Algal Polysaccharides: Nature's Versatile Biopolymers. In Harish & S. Sabiu (Eds.), *Algae and Algal Metabolites* (pp. 1–36). Cham: Springer Nature Switzerland. https://doi.org/10.1007/978-3-031-80866-1_11-1
23. Wang, Z.-Y., Liu, J., Zhu, Z., Su, C.-F., Sreenivasmurthy, S. G., Iyaswamy, A., … Li, M. (2021). Traditional Chinese medicine compounds regulate autophagy for treating neurodegenerative disease: A mechanism review. *Biomedicine & Pharmacotherapy*, *133*, 110968. https://doi.org/10.1016/j.biopha.2020.110968
24. Rathnayake, A. U., Abuine, R., Kim, Y.-J., & Byun, H.-G. (2019). Anti-Alzheimer's Materials Isolated from Marine Bio-resources: A Review. *Current Alzheimer Research*, *16*(10), 895–906. https://doi.org/10.2174/1567205016666191024144044

25. Choudhary, S., Save, S. N., & Vavilala, S. L. (2018). Unravelling the inhibitory activity of Chlamydomonas reinhardtii sulfated polysaccharides against α-Synuclein fibrillation. *Scientific Reports*, *8*(1), 5692. https://doi.org/10.1038/s41598-018-24079-7
26. Panigrahi, G. P., Rane, A. R., Vavilala, S. L., & Choudhary, S. (2019). Deciphering the anti-Parkinson's activity of sulphated polysaccharides from Chlamydomonas reinhardtii on the α-Synuclein mutants A30P, A53T, E46K, E57K and E35K. *The Journal of Biochemistry*, *166*(6), 463–474. https://doi.org/10.1093/jb/mvz064
27. Lucena, A. M. M., De Souza Lucena, E. E., Neto, S. P. D., Nobre, L. T. D. B., Rocha, H. A. O., & Câmara, R. B. G. (2024). Algal polysaccharides: new perspectives for the treatment of basal ganglia neurodegenerative diseases. *Frontiers in Neuroanatomy*, *18*, 1465421. https://doi.org/10.3389/fnana.2024.1465421
28. Yuan, L., Liu, C., Li, B., Wang, S., Zhang, H., Sun, J., & Mao, X. (2024). A green extraction method for agar with improved thermal stability and water holding capacity. *International Journal of Biological Macromolecules*, *278*(Pt 3), 134663. https://doi.org/10.1016/j.ijbiomac.2024.134663
29. Morris, D. L. (1948). Quantitative Determination of Carbohydrates With Dreywood's Anthrone Reagent. *Science*, *107*(2775), 254–255. https://doi.org/10.1126/science.107.2775.254
30. Lowry, O. H., Rosebrough, N. J., Farr, A. L., & Randall, RoseJ. (1951). Protein measurement with the Folin phenol reagent. *Journal of Biological Chemistry*, *193*(1), 265–275. https://doi.org/10.1016/S0021-9258(19)52451-6
31. Torres, P. B., Nagai, A., Jara, C. E. P., Santos, J. P., Chow, F., & Santos, D. Y. A. C. D. (2021). Determination of sulfate in algal polysaccharide samples: a step-by-step protocol using microplate reader. *Ocean and Coastal Research*, *69*, e21021. https://doi.org/10.1590/2675-2824069.21-010pbt
32. Blumenkrantz, N., & Asboe-Hansen, G. (1973). New method for quantitative determination of uronic acids. *Analytical Biochemistry*, *54*(2), 484–489. https://doi.org/10.1016/0003-2697(73)90377-1
33. Dodgson, K., & Price, R. (1962). A note on the determination of the ester sulphate content of sulphated polysaccharides. *Biochemical Journal*, *84*(1), 106–110. https://doi.org/10.1042/bj0840106
34. Freshney's culture of animal cells : a manual of basic technique and specialized applications - National Library of Medicine Institution. (n.d.). Retrieved October 1, 2026, from

https://catalog.nlm.nih.gov/discovery/fulldisplay/alma9918751762106676/01NLM_INST:01NLM_INST

35. Shipley, M. M., Mangold, C. A., & Szpara, M. L. (2016). Differentiation of the SH-SY5Y Human Neuroblastoma Cell Line. *Journal of Visualized Experiments*, (108), 53193. https://doi.org/10.3791/53193
36. Wu, D., & Yotnda, P. (2011). Induction and Testing of Hypoxia in Cell Culture. *Journal of Visualized Experiments*, (54), 2899. https://doi.org/10.3791/2899
37. Cockova, Z., Ujcikova, H., Telensky, P., & Novotny, J. (2019). Protein profiling of SH-SY5Y neuroblastoma cells: The effect of rhein. *Journal of Biosciences*, *44*(4), 88. https://doi.org/10.1007/s12038-019-9908-0
38. Lettieri, M., Emanuele, R., Scarano, S., Palladino, P., & Minunni, M. (2022). Melanochrome-based colorimetric assay for quantitative detection of levodopa in co-presence of carbidopa and its application to relevant anti-Parkinson drugs. *Analytical and Bioanalytical Chemistry*, *414*(4), 1713–1722. https://doi.org/10.1007/s00216-021-03804-8
39. El-Kommos, M. (1990). Spectrophotometric determination of epinephrine and norepinephrine with sodium periodate. *Talanta*, *37*(6), 625–627. https://doi.org/10.1016/0039-9140(90)80206-U
40. Jin, Q., Shan, L., Yue, J., & Wang, X. (2008). Spectrophotometric determination of total serotonin derivatives in the safflower seeds with Ehrlich's reagent and the underlying color reaction mechanism. *Food Chemistry*, *108*(2), 779–783. https://doi.org/10.1016/j.foodchem.2007.11.022
41. Bonting, S. L., Caravaggio, L. L., & Hawkins, N. M. (1963). Studies on sodium-potassium-activated adenosinetriphosphatase. VI. Its role in cation transport in the lens of cat, calf and rabbit. *Archives of Biochemistry and Biophysics*, *101*(1), 47–55. https://doi.org/10.1016/0003-9861(63)90532-0
42. Ellman, G. L., Courtney, K. D., Andres, V., & Featherstone, R. M. (1961). A new and rapid colorimetric determination of acetylcholinesterase activity. *Biochemical Pharmacology*, *7*(2), 88–95. https://doi.org/10.1016/0006-2952(61)90145-9
43. Akter, A., Sobuj, M. K. A., Islam, Md. S., Chakroborty, K., Tasnim, N., Ayon, M. H., … Rafiquzzaman, S. M. (2024). Seaweed polysaccharides: Sources, structure and biomedical applications with special emphasis on antiviral potentials. *Future Foods*, *10*, 100440. https://doi.org/10.1016/j.fufo.2024.100440

44. Holdt, S. L., & Kraan, S. (2011). Bioactive compounds in seaweed: functional food applications and legislation. *Journal of Applied Phycology*, *23*(3), 543–597. https://doi.org/10.1007/s10811-010-9632-5
45. Pereira, L., & Valado, A. (2025). Beyond Nutrition: The Therapeutic Promise of Seaweed-Derived Polysaccharides Against Bacterial and Viral Threats. *Marine Drugs*, *23*(10), 407. https://doi.org/10.3390/md23100407
46. Dhahri, M., Alghrably, M., Mohammed, H. A., Badshah, S. L., Noreen, N., Mouffouk, F., … Emwas, A.-H. (2021). Natural Polysaccharides as Preventive and Therapeutic Horizon for Neurodegenerative Diseases. *Pharmaceutics*, *14*(1), 1. https://doi.org/10.3390/pharmaceutics14010001
47. Preston, M. (2011). Neural stem cell niches: Roles for the hyaluronan-based extracellular matrix. *Frontiers in Bioscience*, *S3*(1), 1165. https://doi.org/10.2741/218
48. Li, S., Zhang, Q., Liu, J., Zhou, X., Wang, N., Chen, H., … Liu, X. (2026). A Novel Polysaccharide (ZJP-2) from Wild Jujube Alleviates Oxidative Damage in Neural Stem Cells: Structural Features and Bioactivity. *Nutrients*, *18*(5), 816. https://doi.org/10.3390/nu18050816
49. Hu, Z., Li, F., Zhou, X., Zhang, F., Huang, L., Gu, B., … Qi, S. (2020). Momordica charantia polysaccharides modulate the differentiation of neural stem cells via SIRT1/B-catenin axis in cerebral ischemia/reperfusion. *Stem Cell Research & Therapy*, *11*(1), 485. https://doi.org/10.1186/s13287-020-02000-2
50. Pomin, V. H., Mahdi, F., Jin, W., Zhang, F., Linhardt, R. J., & Paris, J. J. (2021). Red Algal Sulfated Galactan Binds and Protects Neural Cells from HIV-1 gp120 and Tat. *Pharmaceuticals*, *14*(8), 714. https://doi.org/10.3390/ph14080714
51. Park, Y. S., Lee, H. S., Won, M. H., Lee, J. H., Lee, S. Y., & Lee, H. Y. (2002). Effect of an exo-polysaccharide from the culture broth of Hericium erinaceus on enhancement of growth and differentiation of rat adrenal nerve cells. *Cytotechnology*, *39*(3), 155–162. https://doi.org/10.1023/A:1023963509393
52. Di Lucente, J., Tena, J., Bai, Y., Shafer, C. C., Mendiola, U. R., Neumann, E. K., … Jin, L.-W. (2025). L -Fucose is a candidate monosaccharide neuromodulator and mitigates Alzheimer's synaptic deficits. *Science Advances*, *11*(45), eadt4123. https://doi.org/10.1126/sciadv.adt4123
53. Zheng, X., Boyer, L., Jin, M., Mertens, J., Kim, Y., Ma, L., … Hunter, T. (2016). Metabolic reprogramming during neuronal differentiation from aerobic glycolysis to neuronal oxidative phosphorylation. *eLife*, *5*, e13374. https://doi.org/10.7554/eLife.13374

54. Purushothaman, A., Sugahara, K., & Faissner, A. (2012). Chondroitin Sulfate "Wobble Motifs" Modulate Maintenance and Differentiation of Neural Stem Cells and Their Progeny. *Journal of Biological Chemistry*, *287*(5), 2935–2942. https://doi.org/10.1074/jbc.R111.298430
55. Herrera, F., Chen, Q., & Schubert, D. (2010). Synergistic Effect of Retinoic Acid and Cytokines on the Regulation of Glial Fibrillary Acidic Protein Expression. *Journal of Biological Chemistry*, *285*(50), 38915–38922. https://doi.org/10.1074/jbc.M110.170274
56. Gao, Y., Zhang, J., Tang, T., & Liu, Z. (2024). Hypoxia Pathways in Parkinson's Disease: From Pathogenesis to Therapeutic Targets. *International Journal of Molecular Sciences*, *25*(19), 10484. https://doi.org/10.3390/ijms251910484
57. Tao, B., Gong, W., Xu, C., Ma, Z., Mei, J., & Chen, M. (2024). The relationship between hypoxia and Alzheimer's disease: an updated review. *Frontiers in Aging Neuroscience*, *16*, 1402774. https://doi.org/10.3389/fnagi.2024.1402774
58. Gross, J., Ungethüm, U., Andreeva, N., Heldt, J., Gao, J., Marschhausen, G., … Andersson, K. (1999). Hypoxia during early developmental period induces long-term changes in the dopamine content and release in a mesencephalic cell culture. *Neuroscience*, *92*(2), 699–704. https://doi.org/10.1016/S0306-4522(98)00760-X
59. Lim, J., Kim, H.-I., Bang, Y., Seol, W., Choi, H.-S., & Choi, H. J. (2015). Hypoxia-inducible factor-1α upregulates tyrosine hydroxylase and dopamine transporter by nuclear receptor ERRγ in SH-SY5Y cells. *NeuroReport*, *26*(6), 380–386. https://doi.org/10.1097/WNR.0000000000000356
60. Tai, T. C., Wong-Faull, D. C., Claycomb, R., & Wong, D. L. (2010). Hypoxia and adrenergic function: Molecular mechanisms related to Egr-1 and Sp1 activation. *Brain Research*, *1353*, 14–27. https://doi.org/10.1016/j.brainres.2010.07.036
61. Kumar, G. K. (2011). Hypoxia. 3. Hypoxia and neurotransmitter synthesis. *American Journal of Physiology-Cell Physiology*, *300*(4), C743–C751. https://doi.org/10.1152/ajpcell.00019.2011
62. Rahman, Md. S., & Thomas, P. (2014). Restoration of tryptophan hydroxylase functions and serotonin content in the Atlantic croaker hypothalamus by antioxidant treatment during hypoxic stress. *Frontiers in Neuroscience*, *8*. https://doi.org/10.3389/fnins.2014.00130
63. Petrushanko, I. Yu., Bogdanov, N. B., Lapina, N., Boldyrev, A. A., Gassmann, M., & Bogdanova, A. Yu. (2007). Oxygen-induced Regulation of Na/K ATPase in Cerebellar Granule Cells. *The Journal of General Physiology*, *130*(4), 389–398. https://doi.org/10.1085/jgp.200709783

64. Peter, M. S., & Simi, S. (2017). Hypoxia Stress Modifies Na^+ /K^+ -ATPase, H^+ /K^+ -ATPase, Na+/NH4+-ATPase, and *nkaα1* Isoform Expression in the Brain of Immune-Challenged Air-Breathing Fish. *Journal of Experimental Neuroscience*, *11*, 1179069517733732. https://doi.org/10.1177/1179069517733732
65. Wheaton, W. W., & Chandel, N. S. (2011). Hypoxia. 2. Hypoxia regulates cellular metabolism. *American Journal of Physiology-Cell Physiology*, *300*(3), C385–C393. https://doi.org/10.1152/ajpcell.00485.2010
66. Garcimartín, A., López-Oliva, M. E., González, M. P., Sánchez-Muniz, F. J., & Benedí, J. (2017). Hydrogen peroxide modifies both activity and isoforms of acetylcholinesterase in human neuroblastoma SH-SY5Y cells. *Redox Biology*, *12*, 719–726. https://doi.org/10.1016/j.redox.2017.04.004
67. Zainuddin, M.-S., Bai Magalingam, K., Pamidi, N., Azman, A. S., & Bhuvanendran, S. (2026). In-vitro modelling of Alzheimer's disease using cholinergic neurons derived from human neuroblastoma (SH-SY5Y) retinoic acid-induced differentiation. *Molecular Biology Reports*, *53*(1), 994. https://doi.org/10.1007/s11033-026-12156-4
68. Gamal-Eldeen, A. M., Raafat, B. M., Alrehaili, A. A., El-Daly, S. M., Hawsawi, N., Banjer, H. J., … Almehmadi, M. M. (2022). Anti-hypoxic Effect of Polysaccharide Extract of Brown Seaweed *Sargassum dentifolium* in Tongue Squamous Cell Carcinoma. *Frontiers in Nutrition*, *9*, 854780. https://doi.org/10.3389/fnut.2022.854780
69. Klein, M. O., Battagello, D. S., Cardoso, A. R., Hauser, D. N., Bittencourt, J. C., & Correa, R. G. (2019). Dopamine: Functions, Signaling, and Association with Neurological Diseases. *Cellular and Molecular Neurobiology*, *39*(1), 31–59. https://doi.org/10.1007/s10571-018-0632-3
70. Teleanu, R. I., Niculescu, A.-G., Roza, E., Vladâcenco, O., Grumezescu, A. M., & Teleanu, D. M. (2022). Neurotransmitters—Key Factors in Neurological and Neurodegenerative Disorders of the Central Nervous System. *International Journal of Molecular Sciences*, *23*(11), 5954. https://doi.org/10.3390/ijms23115954
71. Gupta, A., & Sharma, B. (2024). A Review on Neurotransmitters: Dopamine & Serotonin. *Pharmaceutics and Pharmacology Research*, *07*(04), 01–05. https://doi.org/10.31579/2693-7247/178
72. Wang, J., Liu, H., Zhang, X., Li, X., Geng, L., Zhang, H., & Zhang, Q. (2017). Sulfated Hetero-Polysaccharides Protect SH-SY5Y Cells from H2O2-Induced Apoptosis by Affecting the PI3K/Akt Signaling Pathway. *Marine Drugs*, *15*(4), 110. https://doi.org/10.3390/md15040110

73. Zheng, M., Fukuda, T., Zhang, S., Wang, Y., Saito, T., Zhou, Y., … Gu, J. (2026). L-fucose administration ameliorates chronic social defeat stress-induced depressive-like behaviors by restoring GDP-fucose biosynthetic activation and core fucosylation. *Frontiers in Immunology*, *17*, 1909378. https://doi.org/10.3389/fimmu.2026.1909378

Acknowledgements

The authors would like to acknowledge the Management and authorities of KET's V. G. Vaze College (Empowered Autonomous), Mumbai for providing necessary infrastructure for conducting the study. We are thankful to the National Centre for Cell Science, Pune for providing the SH-SY5Y cell line. We are also grateful to Dr. Sukumar Bhakta, Scientist-B, Botanical Survey of India, Kolkata for identification and taxonomic authentication of *Phormidium persicinum* (Reinke) Gom.

Funding

This research did not receive any specific grant from funding agencies in the public, commercial, or not-for-profit sectors.

Author information

Authors and Affiliations

Department of Zoology, KET's V. G. Vaze College (Empowered Autonomous), Mumbai - 400081, Maharashtra, India

Sanjivani Satpute, Thangajyothi Nadar, Kishan Kannaujiya, Akshay Bagwe, Bharatbhushan Sharma

Department of Botany, KET's V. G. Vaze College (Empowered Autonomous), Mumbai - 400081, Maharashtra, India

Manjushri Deodhar

Author Contributions

SS: Data Curation, Formal analysis, Investigation, Methodology, Writing - Original Draft; **TN:** Data Curation, Formal analysis, Investigation; **KK:** Data Curation, Formal analysis, Investigation; **AB:** Conceptualisation, Methodology, Validation, Writing - Review & Editing, Supervision; **MD:** Conceptualisation, Resources, Supervision; **BS:** Project administration, Supervision

Ethics declarations:

Ethics Approval and Consent to Participate

Not Applicable.

Consent for Publication

Not Applicable.

Conflict of interest

The authors declare no competing interests.

Supplementary Files

This is a list of supplementary files associated with this preprint. Click to download.

- Supportingdocument.docx